

## Accepted Manuscript

Research paper

Bi-nuclear luminescent Europium(III) molecular complexes for white light emitting diodes: Experimental and theoretical study

Rajamouli Boddula, Sivakumar Vaidyanathan

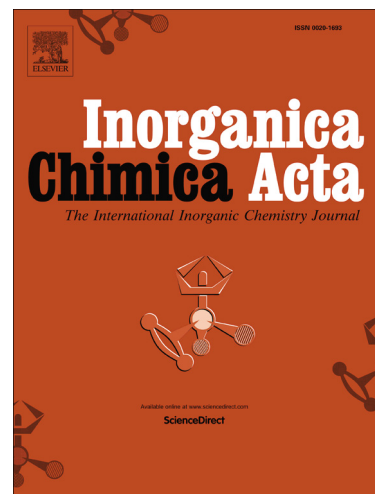
PII: S0020-1693(19)30528-6  
DOI: <https://doi.org/10.1016/j.ica.2019.05.014>  
Reference: ICA 18915

To appear in: *Inorganica Chimica Acta*

Received Date: 16 April 2019  
Revised Date: 8 May 2019  
Accepted Date: 8 May 2019

Please cite this article as: R. Boddula, S. Vaidyanathan, Bi-nuclear luminescent Europium(III) molecular complexes for white light emitting diodes: Experimental and theoretical study, *Inorganica Chimica Acta* (2019), doi: <https://doi.org/10.1016/j.ica.2019.05.014>

This is a PDF file of an unedited manuscript that has been accepted for publication. As a service to our customers we are providing this early version of the manuscript. The manuscript will undergo copyediting, typesetting, and review of the resulting proof before it is published in its final form. Please note that during the production process errors may be discovered which could affect the content, and all legal disclaimers that apply to the journal pertain.



**Bi-nuclear luminescent Europium(III) molecular complexes for white light emitting diodes: Experimental and theoretical study**

Rajamouli Boddula, and Sivakumar Vaidyanathan \*

Department of Chemistry, National Institute of Technology Rourkela, Rourkela-769 008,  
Odisha, India.

---

\* To whom correspondence should be addressed. Email: [vsiva@nitrkl.ac.in](mailto:vsiva@nitrkl.ac.in) (V. Sivakumar)  
Tel: +91-661-2462654;

**Abstract**

Two newly designed and synthesized ancillary ligands with N1 functionalization (phenyl and fluorene) and its influence on photophysical properties of their corresponding binuclear europium complexes were investigated systematically. Photoluminescence (PL) emission spectral study was shown dominant electric dipole transition of  $\text{Eu}^{\text{III}}$  ion ( ${}^5\text{D}_0 \rightarrow {}^7\text{F}_2$ ) and it is clearly indicated that the  $\text{Eu}^{\text{III}}$  ion occupies in the non-centrosymmetric site. The calculated parameter via Judd-Ofelt shown ligands are the best sensitizer for  $\text{Eu}^{\text{III}}$  metal ion. In addition, there is no emission in the region of 400-550 nm (belongs to ligand), indicates that the efficient energy transfer from ligand to central  $\text{Eu}^{\text{III}}$  ion in the complex. The energy transfer mechanism was proposed by the help of DFT and TD-DFT calculations. The obtained highest QY (59.5 %, thin film) of the complex,  $\text{Eu}_2(\text{TTA})_6(\text{L}2)$  indicating efficient energy sensitization from fluorene-based ligand than that of phenyl based Eu-complex. The calculated CIE color coordinates are well matched with NTSC standard values. The binuclear Eu-complexes were combined with InGaN near UV LED, obtained pure red emission (forward bias 20 mA) with CIE color coordinate value  $x = 0.65$ ,  $y = 0.34$  and  $x = 0.66$ ,  $y = 0.33$  for  $\text{Eu}_2(\text{TTA})_6(\text{L}1)$  and  $\text{Eu}_2(\text{TTA})_6(\text{L}2)$ , respectively.

**Key words:** Europium luminescence, spacer molecule, bi-nuclear complex.

## Introduction

Brilliant luminescent performances of molecular lanthanide complexes have been widely studied due to their line like and long life (lifetime ranging from  $\mu\text{s}$ – $\text{ms}$ ) emission ranging from visible and Near-IR region, which are caused by an inter and/or intramolecular energy transfer from the coordinated ligands to the central metal ions [1-3]. In general, the sensitized lanthanide luminescence is highly essential (due to low absorption strength/coefficients of lanthanide ions) and it arises from the singlet excited state or intra-ligand charge transfer states, the antenna chromophore-centred triplet state (the most frequently encountered mechanism), which consequently must be higher in energy than the lanthanide excited emissive state (triplet energies of the well-known ligands are hexafluoroacetylacetonate (hfa,  $22,000\text{ cm}^{-1}$ ), benzoyltrifluoroacetylacetonate (bfa,  $21,400\text{ cm}^{-1}$ ), dibenzoylmethane (dbm,  $20,600\text{ cm}^{-1}$ ), 1,10-phenanthroline (phen,  $21,480\text{ cm}^{-1}$ ) and tetraazatriphenylene (aza,  $23,800\text{ cm}^{-1}$ ) [4-8]. This constrains the range of chromophores that can be used to sensitize lanthanide ions that emit in the visible spectral region.  $\beta$ -diketonates and aromatic N-donor ligands have recognized to be efficient chelators and/ sensitizers of lanthanide emission [9-10]. Design of white light emitting molecular lanthanide complexes are major importance and have attracted recent years by many researchers, because of their potential applications in smart lighting and display devices [11-15].

Careful ancillary or anionic ligand engineering (increase in absorption (oscillator strength) at the wavelength of interest) enables the design of molecular lanthanide complexes leads to red emission with a high quantum yield (efficient energy transfer from ligand to Ln ion) and tunable emission (partial or incompetent energy transfer). Shielding of lanthanide coordination environment by ligand is highly necessary, to prevent the non-radiative transition of lanthanides excited state, induced by high-

frequency oscillators, like the O–H and C–H vibrations of the solvent (play a vital role in reducing the overall quantum yield) [16-17]. Previously we have reported, designing of bipolar ligand and their influence on PL properties of Eu<sup>III</sup> ions and explored their applications in the field of solid-state lighting [18-22]. One of our recent contributions, we have explored phenanthroimidazole-CBZ based bipolar ligand for Eu(III) complex with ethoxy spacer molecule [21].

In the present investigation, we designed and synthesized two new phenanthroline based ancillary ligands (two phenanthroimidazole rings separated by phenyl and ethoxy chain, functionalized in the N1 position with phenyl and fluorene group) and used the same for the synthesis of binuclear Eu-complexes. The luminescent europium site isolation (can prevent concentration quenching effect) can be achieved by using the long ethoxy chain (O-C<sub>4</sub>H<sub>8</sub>-O) along with phenyl (Ph) group. We have shown that the new two binuclear Eu-complex, thereafter labeled Eu<sub>2</sub>(TTA)<sub>3</sub>(L1), Eu<sub>2</sub>(TTA)<sub>3</sub>(L2) allows both PL and EL show characteristic red emission. The majority of the mononuclear Eu-complexes are proved to be the best materials, however, some of the bi and trinuclear Eu-complexes are shown the finest results. As compared with some of the mononuclear complexes, the dinuclear complex offers better thermal stability and stronger luminescence (enhanced QY), which makes it a promising light-conversion molecular device [23-25]. Some of the literature work [26-30] shown that the quantum efficiencies of the bi and trinuclear europium complexes are higher (about 10%) than that of mononuclear ones. In addition, their lifetime of these europium complexes was longer than the mononuclear ones. The chosen Phenanthroline moiety is a rigid planar, hydrophobic, electron-accepting hetero aromatic system, whose nitrogen atoms act cooperatively in cation binding for Eu-metal ion. In addition, it can reduce the non-radiative decay of the excited states of the

europium ion and improve the stability of the europium complexes. It can also benefit to improve the thermal stability of the complex [31]. The chosen flexible alkyl spacer molecule (C-C bond) can make the flexible nature in the complex and may affect on stability [32]. It can also be used to arrest the electronic communication between the two phenanthroimidazole moieties to get efficient emission from the Eu-complexes [21, 33, 34].

Both the ligands and their binuclear Eu-complexes were characterized by various spectroscopic techniques (NMR, FT-IR, Mass and elemental analysis). The ligand structures were optimized by using DFT calculations and their excited state photophysical properties were evaluated by time-dependent density functional theory (TD-DFT) calculation. The designed and synthesized ancillary ligands (L1 and L2) and the corresponding binuclear Eu(III) complex ( $\text{Eu}_2(\text{TTA})_3(\text{L1})$ ,  $\text{Eu}_2(\text{TTA})_3(\text{L2})$ ) molecular structure is depicted in Fig. 1.

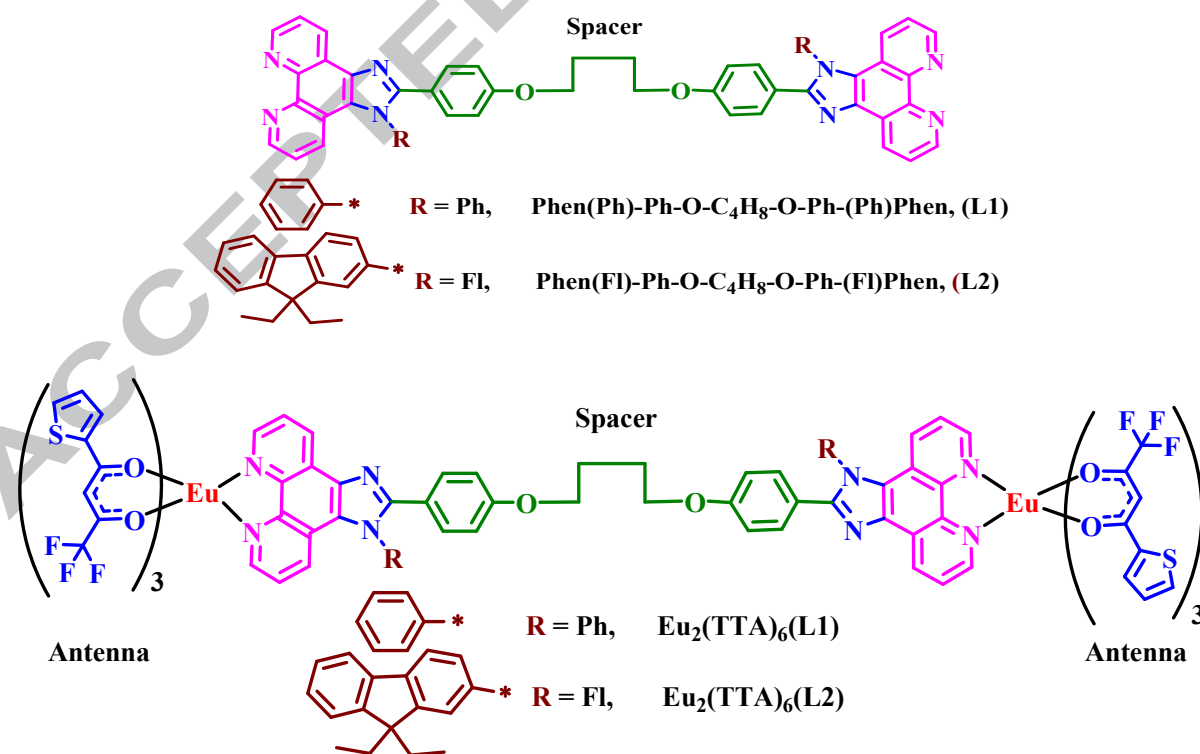
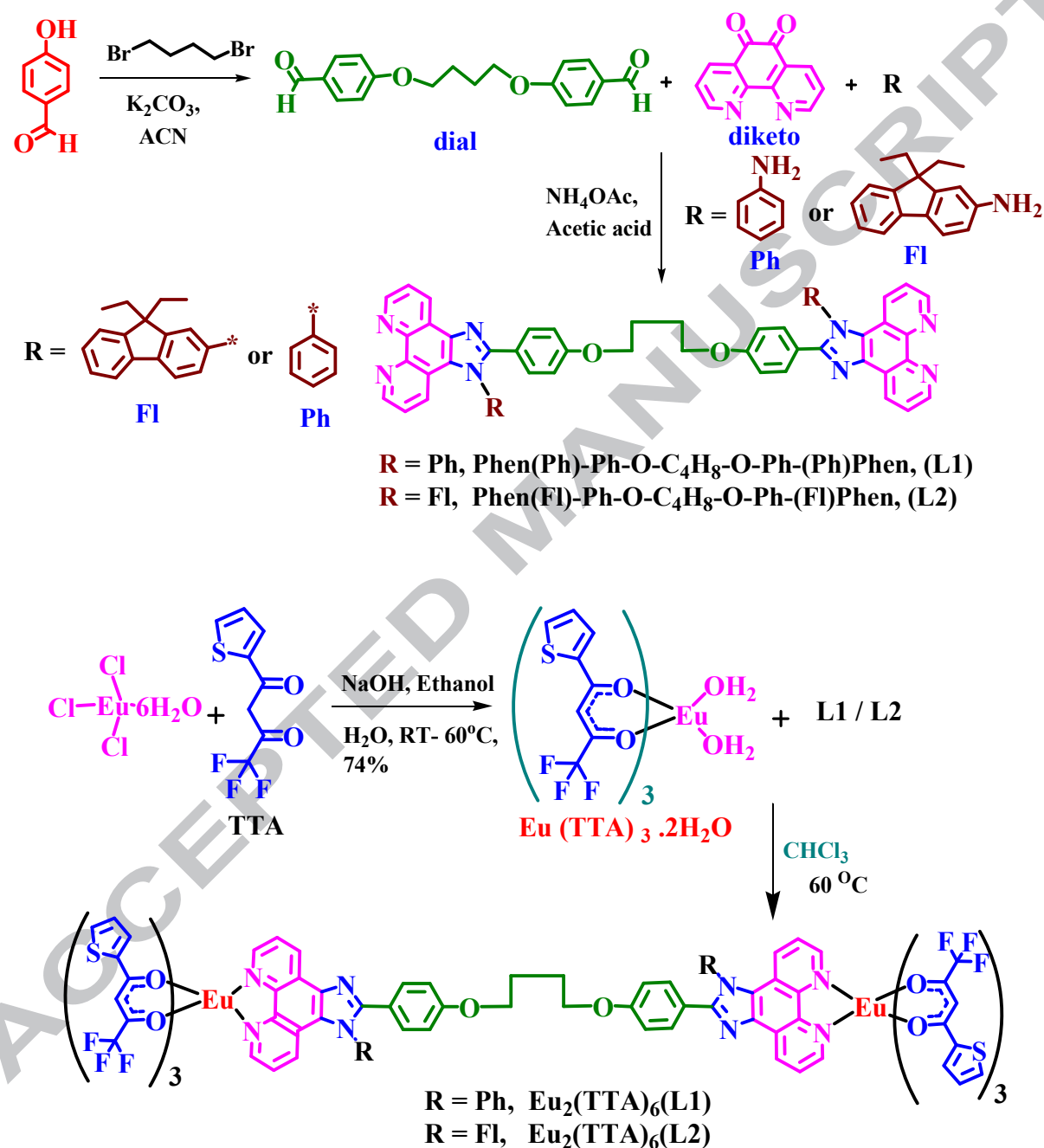


**Fig. 1.** Chemical structure of bipolar ligand and the corresponding binuclear  $\text{Eu}(\text{TTA})_3$  complex.

### Characterization of the complexes

The detailed synthetic condition and reactions of ligands and their binuclear Eu(III) complexes are summarized in Scheme 1.



**Scheme 1.** Synthetic route of the spacer(ether) attached and N1-functionalized phenthroimidazole ligand and the corresponding  $\beta$ -diketonateEu(III) ternary binuclear complex.

## Experimental

**Materials:** The compounds 4-hydroxybenzaldehyde (starting material), aniline and 1,4-dibromom butane, 1, 10-phenanthroline, fluorene and thenoyltrifluoroacetone (TTA) and europium chloride hexahydrate (99.99%) and tetrabutylammonium perchlorate ( $n\text{Bu}_4\text{NClO}_4$ ) electrolyte were purchased from Sigma-Aldrich chemicals company. All the reactions were monitored by thin-layer chromatography (TLC) with silica gel 60 F<sub>254</sub> Aluminium plates (Merk). Column chromatography was carried out using silica gel from Aldrich (70 – 230 mesh, 60 Å). The solvents (tetrahydrofuran, ethanol, dimethyl sulfoxide, hexane etc.) which are used in the current study were carefully dried and distilled from appropriate drying agents prior to use.

**Measurements:** <sup>1</sup>H- and <sup>13</sup>C-NMR spectra were recorded using an AV 400 Avance-III 400MHz Fourier Transform nuclear magnetic resonance (FT-NMR) Spectrometer Bruker Biospin International, Switzerland, in deuterated chloroform/dimethyl sulfoxide solution. Chemical shifts were quoted relative to tetramethylsilane (TMS, standard reference). Fourier Transform infrared (FT-IR) spectra were recorded on a Perkin-Elmer, USA/ RX-I FTIR spectrophotometer and elemental analyses were measured by Elementar Analysen Systeme, Germany/Vario EL spectrometer. Mass spectra were recorded by using LC-Mass spectrometry (Perkin Elmer, USA/ Flexer SQ 300 M). Powder X-ray diffraction of ligand and the Eu(III) complex were measured by powder X-ray diffractometer (XRD) using  $\text{Cu-K}\alpha_1$  radiation (Rigaku, ULTIMA IV). DSC-TGA (thermal decomposition) was performed by using Netzsch, Germany, STA449C/4/MFC/G. The absorption spectrum in solution, solid (Diffuse reflectance spectroscopy, DRS) and thin film were measured by using UV-Visible spectrometer (Shimadzu Corporation, Japan or UV-2450 Perkin Elmer, USA/Lamda 25 and Lamda Perkin Elmer). The PL emission spectrum in solution phase and thin film were recorded by HoribaJobinYvon, USA/Fluoromax 4P spectrophotometer. The CIE coordinates

were calculated by using PL emission data with the help of MATLAB software. The electrochemical properties of the complex and ligand were measured by using cyclic voltammetry (CV), AUTOLAB 302N Modular potentiostat at RT in dichloromethane. The working (glass-carbon rod), auxiliary (counter, Pt wire) and reference (Ag/AgCl wire) electrodes were used for CV analysis. The dichloromethane which contains 0.1 M  $\text{Bu}_4\text{NClO}_4$  was used as the supporting electrolyte and scan rate was maintained as  $100 \text{ mV s}^{-1}$ . The ligand was optimized within density functional theory (DFT) framework using B3LYP/6-31G(d, p) level of theory. After conforming the ground state geometry for the ligand we have vertically excited the molecule to get the UV-Visible spectra and first excited state using TD-DFT. To understand PL spectra of the Eu(III) complex, triplet excited state of the ligand is also obtained by using the same methodology mentioned above. The optimization of the ligand structures was carried out in a G09W suit of the program. The triplet energy of the synthesized ligand was estimated by measuring the phosphorescence spectra of the ligand (Gd-complex) at 77 K by using Edinburgh FLS 920 spectrofluorimeter, UK system consists of a 450 w Xenon lamp (Xe 900) mounted in an air-cooled lamp housing with a built-in de-ozonizer filter. The ozone free Xe arc lamp emits continuous radiation from 190 to 2600 nm. A lifetime of the Eu(III) complex, as well as ligand, were measured at 298 K with Edinburgh Instruments FLS 980 based on the time-correlated single photon counting technology upon the excitation at 360 nm for complexes. A pulsed xenon lamp was used as the excitation source and the signals were detected with a photomultiplier. The solution and solid QY of the complexes were measured by using Edinburgh spectrofluorometer FS5 (integrating sphere).

**Synthesis:** The intermediate compounds are synthesized according to the previously reported literature [16,17]. 9,9-diethyl-9H-fluoren-2-amine (Fl), 1,10-phenanthroline-5,6-dione and the metal compound tris(thenoyltrifluoroacetone)europium (III) ( $\text{Eu}(\text{TTA})_3 \cdot 2\text{H}_2\text{O}$ ) was synthesized by using the well-known method.

**Synthesis of di-aldehyde(dial) compound:**

4-hydroxybenzaldehyde was taken in a round bottom flask and added acetonitrile (CH<sub>3</sub>CN) solution. To this reaction mixture added potassium carbonate base and stirred for 10 minutes then added 1, 4-dibromo butane. The resulting reaction mixture was stirred for 48h at 85 °C under nitrogen atmosphere. The resulting of the reaction mixture was checked by TLC (ethyl acetate (EtOAc) in pet ether 2:8, Rf-0.3). The resulting of the compound was filtered to remove the excess of the base from the reaction mixture. After that, the reaction mixture was extracted with ethyl acetate and followed by dried with anhydrous sodium sulphate. The solvent was evaporated to get 8 g crude compound. The obtained crude was purified by column chromatography by using silica gel (100-200 mesh), eluent with 15 % ethyl acetate in pet ether. The obtained pale yellow color solid was 6.1 g (50.0 %). <sup>1</sup>H-NMR Data (400 MHz, DMSO-d<sub>6</sub>): δ 9.89 (s, 2H), 7.86-7.84 (m, 4H), 7.02-7.00 (m, 4H), 4.16-4.13 (m, 4H), 2.07-2.04 (m, 4H). <sup>13</sup>C-NMR Data (100 MHz, DMSO-d<sub>6</sub>): δ 190.8, 163.9, 132.0, 129.9, 114.7, 67.7, 25.7.

**Synthesis of 2-(4-(4-(4-(1-phenyl-1H-imidazo[4,5-f][1,10]phenanthrolin-2-yl)phenoxy)butoxy)phenyl)-1-phenyl-1H-imidazo[4,5-f][1,10]phenanthroline (L1):**

The aniline (0.122mL, 13.42mmol) was taken in a round bottom flask and added dial compound (2.0 g, 6.771mmol) in glacial acetic acid (30 mL) at room temperature. To this reaction mixture subsequently, ammonium acetate (5.16 g, 67.11mmol) and diketo compound (2.81 g, 13.42mmol) were added. The resulting mixture was stirred for 12 hrs at 110 °C under nitrogen atmosphere. The resulting of the reaction mixture of was monitored by TLC (MeOH in Chloroform 1:9, Rf-0.4). The RM was poured into the minimum amount of water and then added the ammonium hydroxide solution to neutralize the reaction mixture (pH ~7). The solid was filtered and dissolved in dichloromethane, followed by dried with anhydrous sodium sulphate. The solvent was evaporated to get 3.50 g crude compound. The obtained

crude was purified by column chromatography by using silica gel (100-200 mesh), eluent with 4% methanol in chloroform. The purified product was dissolved in minimum amount of THF solution added an excess of hexane solvent, the pale yellow color solid was formed is 400 mg (55.0%). <sup>1</sup>H-NMR Data (400 MHz, DMSO-d<sub>6</sub>): δ 9.08 (dd, 2H, J = 2 Hz, J = 4.4 Hz), 9.01 (dd, 2H, J = 1.6 Hz, J = 8 Hz), 8.94 (dd, 2H, J = 1.6 Hz, J = 4 Hz), 7.87-7.84 (m, 2H), 7.75-7.69 (m, 10H), 7.51 (d, 4H, J = 8.8 Hz), 7.48-7.45 (m, 2H), 7.33 (dd, 2H, J = 1.2 Hz, J = 8.4 Hz), 6.91 (d, 4H, J = 8.8 Hz), 4.04 (br-s, 4H), 1.85 (br-s, 4H). <sup>13</sup>C-NMR Data (100 MHz, DMSO-d<sub>6</sub>): δ 160.1, 153.0, 148.8, 144.3, 138.0, 130.9, 130.9, 129.3, 126.8, 124.1, 122.8, 122.2, 121.0, 114.6, 67.5, 25.4. Elemental analysis: Anal. Calc. for C<sub>54</sub>H<sub>38</sub>N<sub>8</sub>O<sub>2</sub>: C, 78.05; H, 4.61; N, 13.49; Found: C, 78.01; H, 4.58; N, 13.53 %. EI-mass: m/z, Cal. 830.93; found 831.52 (M+1).

**Synthesis of 2-(4-(4-(4-(1-(9,9-diethyl-9H-fluoren-7-yl)-1H-imidazo[4,5-f][1,10]phenanthroline-2-yl)phenoxy)butoxy)phenyl)-1-(9,9-diethyl-9H-fluoren-7-yl)-1H-imidazo[4,5-f][1,10]phenanthroline (L2):**

The same procedure which is followed for the L1 was carried out for synthesis of the ligand L2. NMR Data (400 MHz, DMSO-d<sub>6</sub>): δ 9.07 (m, 1H), 9.01 (d, 1H, J = 8 Hz), 8.91 (d, 1H, J = 4 Hz), 8.17-8.10 (m, 1H), 7.99-7.97 (m, 1H), 7.89-7.87 (m, 2H), 7.68-7.62 (m, 1H), 7.55 (d, 2H, J = 9.2 Hz), 7.49-7.47 (m, 2H), 7.42-7.38 (m, 3H), 6.81 (dd, 2H, J = 2.4 Hz, J = 8.8 Hz), 3.95-3.94 (m, 2H), 3.80-3.79 (m, 1H), 3.68-3.65 (m, 1H), 2.03-2.00 (m, 4H), 0.32-0.28 (m, 3H), 0.16-0.11 (m, 3H). <sup>13</sup>C-NMR Data (100 MHz, DMSO-d<sub>6</sub>): δ 165.0, 159.7, 152.3, 152.2, 150.3, 148.8, 147.9, 144.1, 143.3, 140.1, 136.9, 135.5, 130.9, 130.1, 128.7, 128.0, 127.8, 127.7, 126.9, 124.3, 124.2, 123.8, 123.4, 122.6, 122.4, 122.1, 121.2, 119.9, 114.5, 97.6, 82.9, 68.7, 67.6, 66.1, 56.75, 33.6, 32.3, 25.5, 23.7, 8.74, 8.51. Elemental analysis: Anal. Calc. for C<sub>76</sub>H<sub>62</sub>N<sub>8</sub>O<sub>2</sub>: C, 81.55; H, 5.58; N, 10.01; Found: C, 81.52; H, 5.52; N, 10.05 %. EI-mass: m/z, Cal. 1118.5; found 1120.24 (M+1).

**Synthesis of  $\text{Eu}_2(\text{TTA})_6(\text{L1})$ :** Taken two neck round bottom flask (50 mL) with nitrogen-containing balloon adaptor and poured  $\text{Eu}(\text{TTA})_3 \cdot 2\text{H}_2\text{O}$  (205 mg, 0.240mmol, 1 eq) dissolved in dry chloroform ( $\text{CHCl}_3$ ) (15 mL). To this solution, an added mixture of compound L1 (200 mg, 0.240mmol, 1eq) in chloroform (10 mL) and the reaction mixture (RM) stirred for 12h at 60 °C temperature. The resulting product was dissolved in a minimum amount of THF and excess of hexane added to get a solid product. The obtained final pale yellow color product was 414 mg (70.0%). Elemental analysis: Anal. Calc. for  $\text{C}_{102}\text{H}_{62}\text{Eu}_2\text{F}_{18}\text{N}_8\text{O}_{14}\text{S}_6$ : C, 49.76; H, 2.54; N, 4.55; S, 7.81; Found: C, 49.72; H, 2.51; N, 4.59; S, 7.84%.

**Synthesis of  $\text{Eu}_2(\text{TTA})_6(\text{L2})$ :**

The same procedure which is followed for the  $\text{Eu}_2(\text{TTA})_6(\text{L1})$  was carried out to the synthesis of the ligand L2. Elemental analysis: Anal. Calc. for  $\text{C}_{124}\text{H}_{86}\text{Eu}_2\text{F}_{18}\text{N}_8\text{O}_{14}\text{S}_6$ : C, 54.15, H, 3.15, N, 4.07, S, 7.00; Found: C, 54.12, H, 3.11, N, 4.02, S, 6.98%.

**FT-Infrared spectroscopy:**

The infrared spectra of the ligands and their complexes were measured in the room temperature in the range of 500 - 4000  $\text{cm}^{-1}$ . The observed major strong carbonyl ( $\text{C}=\text{O}$ ) stretching frequency fictional group of  $\text{Eu}(\text{TTA})_3 \cdot 2\text{H}_2\text{O}$  complex found to be at 1614  $\text{cm}^{-1}$  and which is shifted to 1601  $\text{cm}^{-1}$  for the  $\text{Eu}_2(\text{TTA})_6(\text{L1})$  and 1599  $\text{cm}^{-1}$  for the  $\text{Eu}_2(\text{TTA})_6(\text{L2})$  (Fig. 2). These changes are the evidence that the  $\beta$ -diketonate ( $\text{Eu}(\text{TTA})_3$ ) compound coordinated with ligand (L1 and L2), respectively. It leads to a form of the  $\text{C}=\text{N}$  bond is converted into a structure of  $\text{C}=\text{N}-\text{Eu}-\text{O}$  bond. In addition, the vibration frequency of  $\text{C}=\text{N}$  appears at 1605  $\text{cm}^{-1}$ (L1) and 1602  $\text{cm}^{-1}$  (L2) in the ligands were shifted to 1538 and 1537  $\text{cm}^{-1}$  in the complex, respectively. These major functional group changing is indicated that the ligand coordinated with Eu(III) ion. Furthered, it was also supported by remained functional groups varying from ligand to complex which are tabulated in the Table 1. These results are concluding that the N atom in ligand coordinates with  $\text{Eu}(\text{TTA})_3$ .

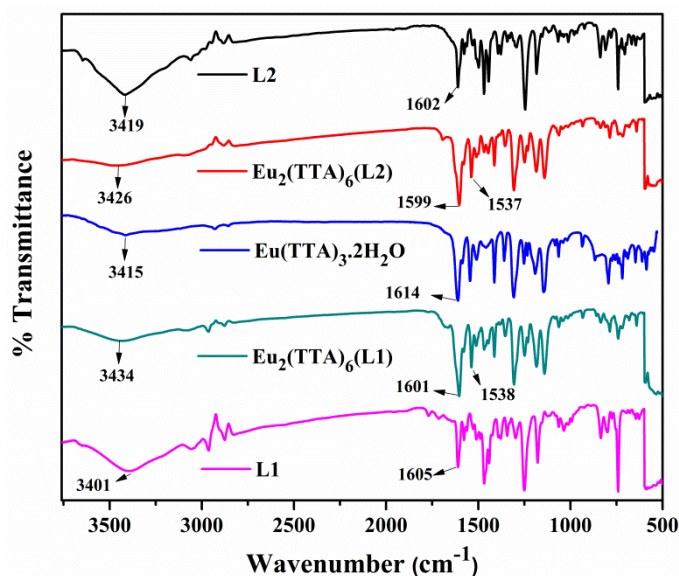


**Fig. 2.** FT-IR spectra of the ligands and corresponding Eu(III)-complexes as well as comparison with  $\text{Eu}(\text{TTA})_3$ .

**Table 1.** The Infrared frequencies (wavenumber in  $\text{cm}^{-1}$ ) at room temperature (RT) for free ligands and its corresponding  $\text{Eu}_2(\text{TTA})_3(\text{L1})$ ,  $\text{Eu}_2(\text{TTA})_3(\text{L2})$  complex and  $\text{Eu}(\text{TTA})_3$ .

(Wavenumber in $\text{cm}^{-1}$ )	$\text{Eu}_2(\text{TTA})_3(\text{L1})$	$\text{Eu}_2(\text{TTA})_3(\text{L2})$	L1	L2	$\text{Eu}(\text{TTA})_3$
$\nu(\text{C}=\text{O})$	1601	1599	---	---	1614
$\nu(\text{C}=\text{N})$	1538	1537	1605	1602	---
$\nu(\text{C}-\text{N})$	1249	1250	1247	1245	---
$\nu(\text{C}-\text{F})$	1307	1306	---	---	1300
$\nu(\text{C}-\text{CF}_3)$	1142	1140	---	---	1137
$\nu(\text{C}-\text{H phen})$	832, 786	835, 785	836, 742	839, 740	---

## Results and Discussion

The synthesis of binuclear Eu-complexes ( $\text{Eu}_2(\text{TTA})_6(\text{L1})$  and  $\text{Eu}_2(\text{TTA})_6(\text{L2})$ ) and their photophysical/luminescent properties were discussed in detail in the results and

discussion part. The effect of N1 functionalization of the ligand by phenyl and fluorene moiety (L1 and L2) and the binuclear Eu-complexation by the same has been achieved. The synthesized ligands and their corresponding binuclear Eu-complexes were characterized by using various spectroscopic techniques (nuclear magnetic resonance spectroscopy ( $^1\text{H}$  and  $^{13}\text{C}$  NMR, Fig. S1-S3), ESI-Mass spectrometry (Fig. S4-S5), Elemental analysis, Fourier transforms infrared spectroscopy (FT-IR), etc). All the measurements were carried out at room temperature (RT). Coordination of the ligand and complex confirmation made by FT-IR and elemental analysis made to confirm the presence of the molecular complex. The thermal decomposition and morphological study of the ligands as well as the corresponding binuclear Eu complexes also been discussed. The synthesized binuclear  $\text{Eu}^{\text{III}}$  complexes were imbedded in a PMMA matrix with different  $\text{Eu}^{\text{III}}$  complex concentrations and studied their photophysical properties. The detailed PL excitation and emission spectra express the essential information regarding the absorption characteristics of the attached chromophoric ligating group and site symmetry with respect to  $\text{Eu}^{\text{III}}$  ion in the complex. The theoretical calculations were performed by using density functional theory (DFT) frame work using B3LYP/6-31G (d, p) level of theory, to estimate the energy levels to support the mechanistic pathway of energy transfer from ligand to Eu ion in the complex.

### **Thermal Properties and Powder X-ray diffraction (PXRD) studies**

The thermal behaviour of the ligand (L1 and L2) and the corresponding binuclear Eu-complex ( $\text{Eu}_2(\text{TTA})_6(\text{L1})$  and  $\text{Eu}_2(\text{TTA})_6(\text{L2})$ ) under a nitrogen atmosphere were examined by means of thermogravimetric analysis (TGA). The general profile of the weight loss for the ligands and the binuclear Eu-complexes are displayed in Fig. 3. The TGA of the complexes,  $\text{Eu}_2(\text{TTA})_6(\text{L1})$  and  $\text{Eu}_2(\text{TTA})_6(\text{L2})$  shown 10 %

decomposition at 283 and 279 °C, respectively. The TGA of the complexes,  $\text{Eu}_2(\text{TTA})_6(\text{L1})$  and  $\text{Eu}_2(\text{TTA})_6(\text{L2})$  are shown first minor mass loss of approximately 6.01 % in the range of 110 to 165 °C which corresponds to the elimination of the coordinated water and solvent molecules. The major second decomposition of the  $\text{Eu}_2(\text{TTA})_6(\text{L1})$  and  $\text{Eu}_2(\text{TTA})_6(\text{L2})$  observed at ~320 °C (lost 12.1 % and reached to 87.8 %) and ~316 °C (lost 11.8 % and reached to 88.1 %), respectively which corresponds to the degradation of the TTA ligands (ranging from 250-320 °C) [35-37]. The third decomposition undergoes at 438 (lost 54 % and reached to 64 %) and 404 °C (lost 61 % and reached 38.9 %) and final decomposition undergoes at 651 and 545 °C, respectively. These correspond to the decomposition of the ancillary ligands (presence of fluorene, Phenyl, phenanthroline groups). The ligand (L1 and L2) thermal decomposition temperature is high as compared with Eu-complexes. The first small decomposition of ligands (L1 and L2) shown at 184 and 170 °C belongs to the water molecules and major decomposition at 403 (lost 8.26 % and reached to 91.7 %) and 417 °C (lost 14.1 % and reached to 85.8 %), respectively. The temperature at 442 and 225 °C observed 10 % weight loss, which is attributed to the decomposition of ligand fragments (fluorene, Phenyl, phenanthroline groups) presence in the ligand. As compared with spacer alkyl chain attached mononuclear substituted Eu-complex consisted of lower thermal stability than the currently synthesized bi-nuclear alkyl chain spacer Eu-complex [21].

The DSC studies of the ligands and the corresponding binuclear complexes show the glass transition temperature ( $T_g$ ) ranging from 137 to 333 °C. The ligand moieties are shown good  $T_g$  values as compared to that of corresponding Eu complexes (the same is marked in the DSC curve in Fig. 3 right). The  $T_g$  of the ligands L1 and L2 are 333 and 235 °C as well as respective complexes,  $\text{Eu}_2(\text{TTA})_6(\text{L1})$  and  $\text{Eu}_2(\text{TTA})_6(\text{L2})$

shown 142 and 137 °C, respectively. The PXRD analysis of the complexes was shown broadband spectra and it is indicating that the amorphous nature of the complexes. The pictorial view of the PXRD and their 2-theta (deg), d (ang.) are tabulated in Fig. S6 and Table S1, S2; respectively.

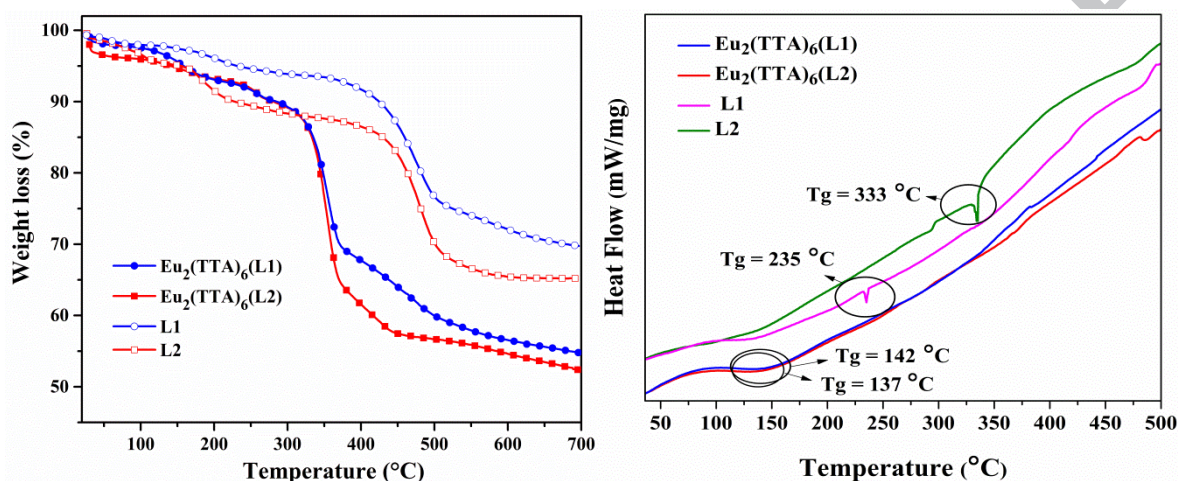


**Fig.3.** TG analysis curves for the ligands (L1 and L2) and its corresponding binuclear Eu(III) complexes ((Eu<sub>2</sub>(TTA)<sub>6</sub>(L1) and Eu<sub>2</sub>(TTA)<sub>6</sub>(L2)) (left) and in onset mentioned their DSC curves (right).

### Photophysical properties

#### UV-Visible absorption and Diffuse Reflectance Spectral studies:

The absorption spectrum of the ligands (L1 and L2) and the corresponding binuclear Eu-complexes is shown in Fig. 4, left. Singlet-singlet  $n-\pi^*$  enolic transition was assigned to the  $\beta$ -diketonate moiety in the complex. Both the ligands and the Eu complex show similar absorption spectral profile, however, the absorption edge of the Eu complex is slightly shifted towards near UV region (extending to a longer wavelength from 350 to 400 nm). In addition, the absorption peak consists shoulder in the near UV region, which is not present in the case of ligands. The strong absorption in the UV-Vis region is due to strong  $\pi$  to  $\pi^*$  transition of aromatic chromophores present in the complex as well as ligand moieties. The occurrence or coordination of the bipolar ligand not only enhances the absorption intensity but also fulfills

the high coordination number of the central metal  $\text{Eu}^{\text{III}}$  ion. Thus, it improves the coordination saturation as well as thermal stabilities of binuclear Eu-complexes. The calculated absorptions peaks are tabulated in Table 2. The band gap was calculated for all the compounds by converting the UV-visible data (Fig. 4, right) into Kubelka-Munk function. The acquired spectrum is converted to Kubelka-Munk function ( $\alpha = F(R_\infty)$ ).<sup>38</sup>

$$\alpha h\nu = A(h\nu - E_g)^n \quad (1)$$

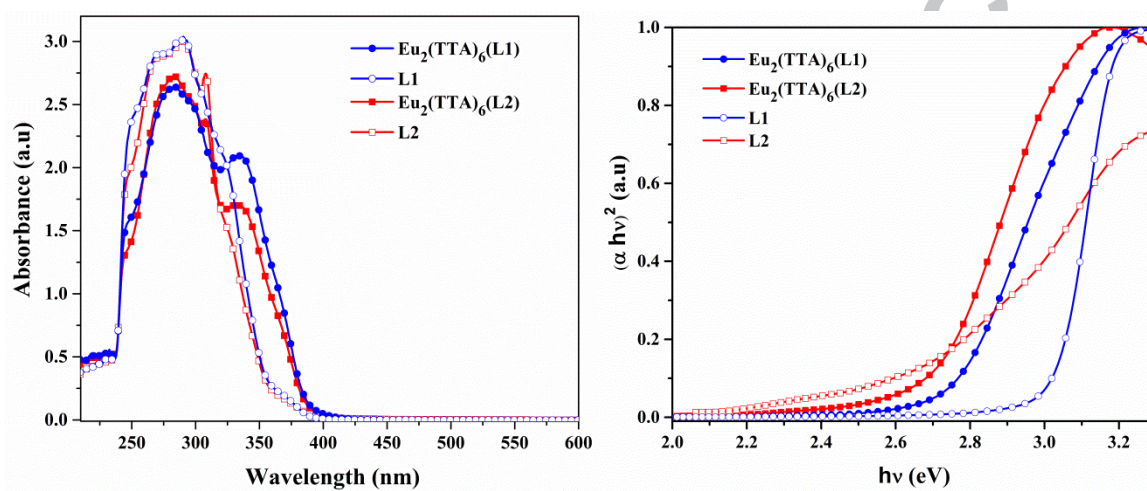


**Fig. 4.** The UV-Visible absorption spectra of the bipolar ligands and corresponding binuclear Eu-complex (left). Bandgap calculations from solid UV-Vis spectra of ligand and complexes (right).

**Table 2.** The UV-absorption and PL emission data of synthesized Eu(III) complexes and ligands.

S. No.	Compound name	UV $\lambda_{\text{max}}$ (abs)[nm]		$\lambda_{\text{ex}}$ [nm] Solution/solid	PL $\lambda_{\text{em}}$ (c) [nm]	FWHM	$I_2/I_1$ ratio
		(a)	(b)				
1.	<b>Eu<sub>2</sub>(TTA)<sub>6</sub>(L1)</b>	246, 284, 335		321, 374 /272,	580, 592, 612,	4.31/4.4	14.2/
				230, 426(d)	652, 702	3(d)	13.8(d)
2.	<b>Eu<sub>2</sub>(TTA)<sub>6</sub>(L2)</b>	245, 285, 335		320, 365/270,	580, 592, 612,	4.78/	16.0/
				230, 438(d)	652, 702	6.26(d)	10.2(d)

3.	<b>L1</b>	249, 269, 290, 324	347/275, 320, 365(d)	425/448(d)	---	---
4.	<b>L2</b>	248, 271, 289, 326	352/276, 315, 365(d)	425/521(d)	---	---
5.	<b>Eu(TTA)<sub>3</sub></b>	273, 340	275, 340	580, 592, 612, 652, 703	~ 6	~11

[a] measured at 298 K in chloroform solution, [b] absorption peaks from the UV-absorption spectra, [c] emission peaks from PL emission spectra, [d] values of compounds in solid.

### Photoluminescence studies:

The synthesized ligand and binuclear Eu<sup>III</sup> complexes PL in solution state excitation spectra in chloroform solvent,  $c = 1 \times 10^{-5}$  M were recorded at room temperature. The ligands, L1 and L2 in solution form are shown emission at a blue region which is 425 nm at excitation wavelength 347 and 352 nm, respectively (Fig. 4). However, the solid of the ligands, L1 and L2 shown emission at 448 and 521 nm with excitation wavelength 365 nm, respectively (Fig. 5). The spectral shifting (bathochromic shift) from the solution to solid was observed is due to aggregation. In the Eu-complexes the excitation spectral profile was taken by monitoring the  $^5D_0 \rightarrow ^7F_2$  (612 nm) electric dipole transition of the Eu<sup>III</sup> ion. The spectra consist of broad absorption in the UV region (broadband between 275 and 450 nm), which can be assigned to the  $\pi-\pi^*$  electronic transition of the aromatic moieties present in the ligand. The absence of f-f transitions of the Eu<sup>III</sup> ion in the absorption spectrum evidence that the luminescence sensitization *via* the excitation of the ligand is effective in the presently studied complexes. In other words it can say that the f-f transition are absent because they are too weak to be observed in a diluted solution.

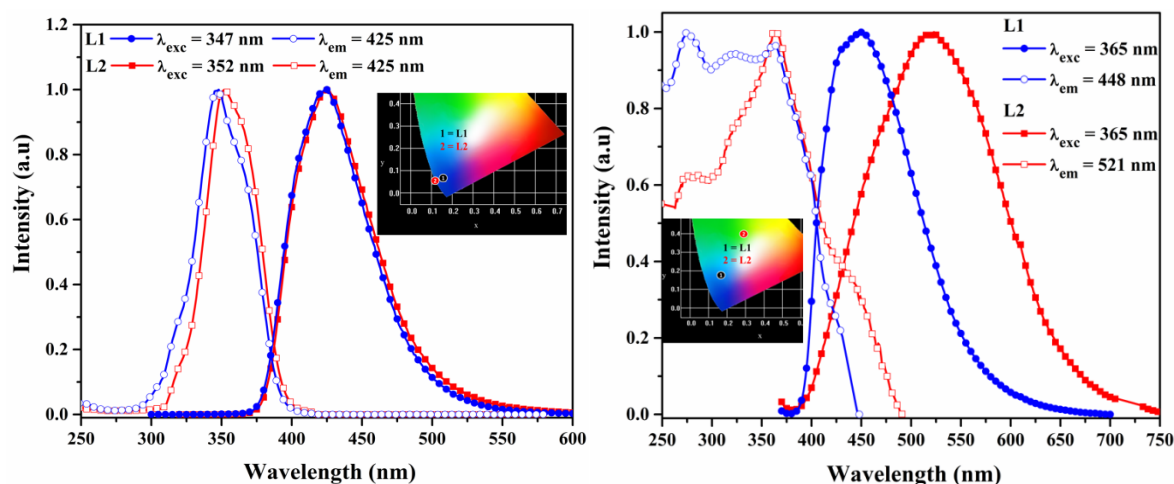


**Fig. 5.** The PL excitation and emission spectra of the ligands (L1 and L2) in solution (left) and solid state (right).

The PL emission of the complexes and ligands were studied in solution and solid phase (Fig. 6). The emission bands of the  $\text{Eu}^{\text{III}}$  complexes are observed at around 579, 592, 612, 650 and 695 nm, and are attributed to the  $^5\text{D}_0 \rightarrow ^7\text{F}_J$  (f-f transitions) with  $J = 0, 1, 2, 3$  and  $4$ , respectively. The  $^5\text{D}_0 \rightarrow ^7\text{F}_0$  transition is weak and situated at 579 nm (single peak) due to  $^5\text{D}_0 \rightarrow ^7\text{F}_0$  transition indicates that all  $\text{Eu}^{\text{III}}$  ions in the structure occupy a site of the same symmetry and experience the similar crystal field perturbation in the complex. The moderately strong  $^5\text{D}_0 \rightarrow ^7\text{F}_1$  transition is indicated when  $\text{Eu}^{\text{III}}$  ion occupies the center of the symmetric site and this magnetic dipole transition is independent of the coordinate environment. The hypersensitive  $^5\text{D}_0 \rightarrow ^7\text{F}_2$  transition (electric dipole) consists of a strong band at 612 nm, it leads to red luminescence of the complex and the local environment of the Eu ion sense to be more non-symmetrical. The observed broad peaks at about 650 as well as 695 nm correspond to the  $\text{D}_0 \rightarrow ^7\text{F}_3$  and  $^5\text{D}_0 \rightarrow ^7\text{F}_4$  transitions, respectively. It is worth to note that the absence of a broad-band in the 380–530 (solution) and 380–700 nm region corresponding to the ligand emission in the emission spectra highlights that

the efficient ligand-to-metal energy transfer occurs in the presently studied Eu-complexes.

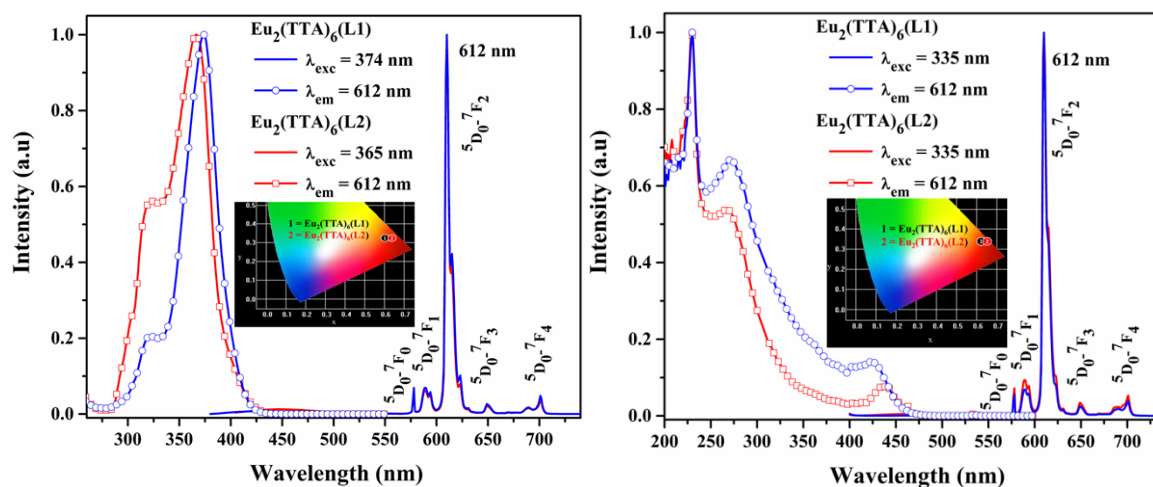


**Fig. 6.** The PL excitation and emission spectra of the binuclear Eu(III) complex in solution (left) and solid state (right).

The intensity of the electric dipole transition is more intense and it reaches the characteristic red emission. The europium ion site symmetry or asymmetric ratio was calculated from the integration emission intensity ratio of the  $^5D_0-^7F_2$  transition to  $^5D_0-^7F_1$  transition ( $I_2/I_1$ ) from the PL emission spectra of the complexes in solution as well as solid. The intensity ratio ( $I_2/I_1$ ) of the Eu(III) complex,  $\text{Eu}_2(\text{TТА})_6(\text{L1})$  in solution and solid are 14.2 and 13.8;  $\text{Eu}_2(\text{TТА})_6(\text{L2})$  in solution and solid are 16.0 and 10.2; respectively. The intensity ratio of the solution was found to be higher than solid. It is also indicating that the Eu(III) ion occupied non-center of symmetry site. In addition, it was clear that the Eu(III) ion and ligand have strong coordination interaction. As compared with the intensity ratio ( $I_2/I_1$ ) of  $\text{Eu}(\text{TТА})_3$  was around 11.5 which is indicating that the current synthesized Eu-complexes are in high-intensity ratio than  $\text{Eu}(\text{TТА})_3$  in solution. The calculated full width at half maximum (FWHM) values are 4.31 and 4.78 nm (solution); 4.43 and 6.26 nm (solid) for  $\text{Eu}_2(\text{TТА})_6(\text{L1})$  and  $\text{Eu}_2(\text{TТА})_6(\text{L2})$ , respectively. The less value of FWHM for the complexes is indicating

that the narrow emission intensive characteristic band is very much suitable to achieve the efficient red emission.

It is generally believed that the energy transfer process proceeds through triplet pathway in the europium luminescent complexes. The energy transfer from ligand to center metal ion is very much necessary to understand the excited energy levels. Since the energy transfer from the organic part towards metal ions occurs efficiently by two different pathways. In which the first one, described by Forster, it takes into an account of multipolar interactions between distinct oscillating centers [39]. The second one is Dexter's mechanism, which can describe as postulates energy transfer as electron exchange between the organic ligand and lanthanide ion [40,41]. The similar nature of this process requires an overlap of the emission spectra of the donor (ligand) and the absorption spectra of the acceptor. Based on these criteria it was examined by the overlap between the emission spectrum of the ligand (L1 and L2) and absorption spectra of the TTA (acceptor). The overlap observed in the region of 375-450 nm. It is clearly indicating that the energy transfer process can appear through ligand triplet to TTA triplet excited state through intramolecular energy transfer [42,43]. The process implicates of photoexcitation of the ligand (antenna or organic chromophore) energy to  $\text{Eu}^{\text{III}}$  ion via their triplet ( $^3\text{T}$ ) states by means of internal conversion; finally, the  $\text{Eu}^{\text{III}}$  ion emits photons to ground state from first excited levels ( $^5\text{D}_0$ ). It is also well documented that the  $\text{Eu}^{\text{III}}$  excited levels were located at  $^5\text{D}_3$  ( $24,800\text{ cm}^{-1}$ ),  $^5\text{D}_2$  ( $21,500\text{ cm}^{-1}$ ), and  $^5\text{D}_1$  ( $19,100\text{ cm}^{-1}$ ), to  $^5\text{D}_0$  ( $17,500\text{ cm}^{-1}$ ) feasible by internal conversion (thermal activation) [44]. The energy level matching is the key factor one need to consider for efficient energy transfer from ligands to  $\text{Eu}^{\text{III}}$  ion in the complex. Thus, the energy level's match of the triplet state of the ligands to  $^5\text{D}_0$  of  $\text{Eu}^{\text{III}}$  is one of the vital factors, which directly influence the PLQY of the Eu complex. It is also well known that anionic ligand (TTA) energy levels located at 25,164 (singlet) and 18,954 (triplet) [19]. The calculated singlet ( $^1\text{S}$ ) and triplet ( $^3\text{T}$ ) energy levels of

the Eu<sup>III</sup> complex by DFT and TD-DFT analysis of L1 and L2 were located at 29,013(3.59 eV), 27,172 (3.36 eV) cm<sup>-1</sup> (singlet) and 22,173(2.74 eV), 22,152 cm<sup>-1</sup> (2.74 eV) (triplet) shown in Fig.7. The triplet levels of the ligands were also calculated by using Gd-complex at 77 K, which results are shown similar to that of the theoretical (Fig. S12). These obtained results are showing capable of transferring the populated energy from the triplet state of the ligand to <sup>5</sup>D<sub>0</sub> of Eu<sup>III</sup> metal ion efficiently. These outcomes were also supported according to the Latvaet *al.*, calculations [9] (( $\Delta E = E(T_1) - E(^5D_0)$  is 2500 - 4000 cm<sup>-1</sup>; singlet above 25,000 (3.09 eV) and triplet above 20,000 cm<sup>-1</sup> (2.47 eV)). Since the energy difference between the <sup>3</sup>T and <sup>5</sup>D<sub>0</sub> level is comparatively high and hence there is no reversible emission possible (due to back transfer) from the complex and the same was reveals in the PL emission spectra (no emission was observed in the range of 400 to 550 nm for ligand moieties). It could be expected that the fluorene in the complex sensitization boosted by decrease the vibronic quenching effect. We have also reported recently the fluorene molecule at the N<sub>1</sub> position in the ligand is better sensitizer than consist of the alkyl chain (ethyl) [21]. The observed complete energy transfer process was also been supported by Reinhoudt's empirical rule [45]. In addition, it was also discussed that in this energy transfer mechanism TTA excited singlet and triplet state can act as a transitional state between the singlet to triplet excited states of the ligand as well as triplet excited state to the excited <sup>5</sup>D<sub>0</sub> level of Eu(III) ion, respectively. The effective overlap between the ligating moieties and the absorption spectrum of TTA showed that the characteristic luminescence of the corresponding Eu<sup>III</sup> occurs through intramolecular energy transfer which is shown in pictorial view in Fig. S7.

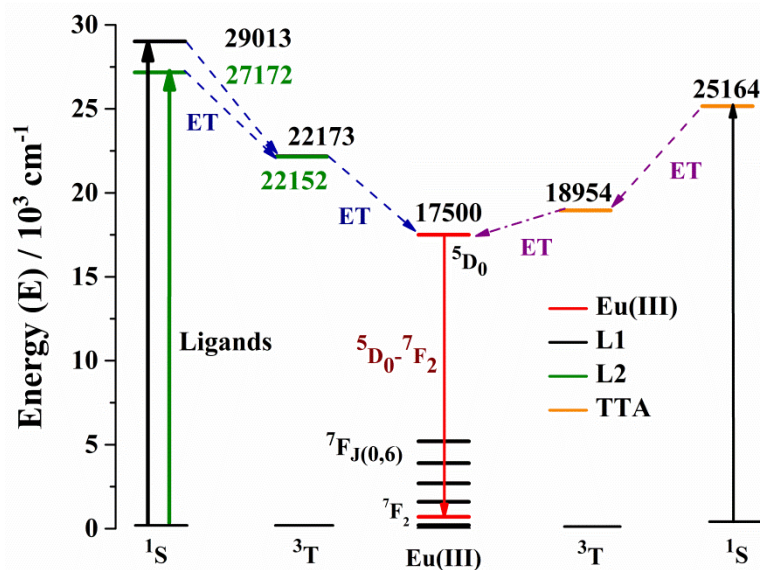


**Fig. 7.** The energy transfer diagram for the complexes and energy transfer to  $\text{Eu}^{\text{III}}$  ion from ligand as well as TTA molecule (S = singlet, T = triplet, ET = energy transfer).

The emission under UV lamp (365 nm) of the ligands and complexes are in solution, thin film and solid form are shown in Fig. 8. The blue color emission was observed from the ligand under the UV lamp, whereas the corresponding Eu complex shown red emission at 365 nm. The respective thin films of the complexes are shown bright red color. The  $\text{Eu}(\text{TTA})_3$  also shown which is shown red color emission.

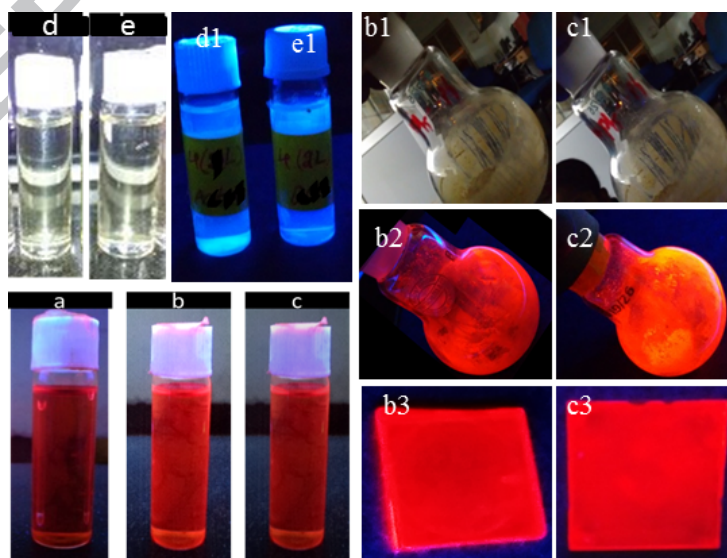


**Fig.8.** Ligands and corresponding  $\text{Eu}(\text{III})$  complexes under UV (365 nm) light are (a)  $\text{Eu}(\text{TTA})_3$ , (b)  $\text{Eu}_2(\text{TTA})_6(\text{L1})$ , (c)  $\text{Eu}_2(\text{TTA})_6(\text{L2})$ ; (b1) (c1) are under normal light; (b2) (c2)

are under UV light; (b3) (c3) are thin films; (d) (e) are L1 and L2 under normal light (d1) (e1) are under UV light.

These obtained outcomes (PLQY) were compared with the unimolecular Eu-complex [21] shown higher QY in the solution state and similar in the case of solid, respectively. The obtained results clearly indicating in solution state the radiative pathway increasing by reducing non-radiative transition. However, in the solid state, there is no effect was found. The detailed calculations of the Eu-complex absolute quantum efficiency (measured by the integration sphere) are reported elsewhere [18, 21]. The absolute quantum efficiency (measured by the integration sphere) of the complex was carried out in solution as well as solid by monitoring the higher electric dipole transition (612 nm). The obtained absolute QY for the binuclear Eu-complex in solution is found to be 40.7 and 30.0 %, respectively. Whereas, the complexes are in solid state show 31.8 and 32.4 %, respectively. In addition, QY of the complexes doping with PMMA thin film was also measured and shown 52.7 and 59.5 %. The observed QY is higher than the solution and solid. It indicates that the PMMA leads to efficient energy transfer via reducing the non-radiative transitions. It is also worth to note that the presence of PMMA matrix leads to closer the acceptor and donor. In addition, QY of the thin film of  $\text{Eu}_2(\text{TTA})_6(\text{L2})$  consists higher than that of  $\text{Eu}_2(\text{TTA})_6(\text{L1})$ . It is expecting due to the presence of fluorene molecule in the complex,  $\text{Eu}_2(\text{TTA})_6(\text{L2})$  leads to increase the efficient energy transfer to center  $\text{Eu}^{\text{III}}$  metal via ligand. The similar observations also found in the case of solid. These results can also support by the theoretical calculations of the singlet and triplet energy levels location and singlet energy level (L1) is near to the triplet level as compared with L1. So it may efficiently transfer energy in L2 than L1 via singlet to triplet energy level. As compared with the reported phenanthroline with spacer consisted complex (solution and solid are 11.5 and 5%) [21], currently synthesized complexes were shown improved QY (solution above 3 times, solid above 6 times). These

results are suggesting that the fluorene with spacer molecule in binuclear complexes (2 Eu metal ions) extensively increase the energy transfer process leads to high QY.

### Judd-Ofelt and Life time analysis

The Judd-Ofelt parameters were essential to understand the physical implication of the symmetric/asymmetric and covalent/ionic bonding environment between Eu(III) ion and the surrounding ligand moiety. Since these calculations were initials to calculate the sensitization energy transfers process and other parameters. The J-O parameters were calculated for Eu(III) complexes to form the PL emission spectra by well-reported method from literature [18,42,46]. The calculated value has been tabulated in Table 3 and the  $\Omega_2$ ,  $\Omega_4$  values are 1.79, 0.23 ( $10^{-20} \text{ cm}^2$ ) ( $\text{Eu}_2(\text{TTA})_6(\text{L1})$ ) and 2.44, 0.244 ( $10^{-20} \text{ cm}^2$ )  $\text{Eu}_2(\text{TTA})_6(\text{L2})$ , respectively. To achieve the best Eu(III) radiative rates, necessary to design asymmetrical Eu(III) complexes with having larger  $\Omega_2$ . Intensity parameter  $\Omega_4$  ( ${}^5\text{D}_0 \rightarrow {}^7\text{F}_2$ ) is less sensitive to the coordination sphere than  $\Omega_2$  in the complex and reflects chemical environment rigidity surrounding the Eu(III) ion. The most important isolated magnetic dipole is  ${}^5\text{D}_0$  to  ${}^7\text{F}_1$  ( $J=1$ ) transition and it has no electric dipole involvement, which is practically independent of the ion's chemical environment. Based on these criteria it can be used as a reference for calculating of J–O intensity parameters.

The lifetime of the ligands, as well as complexes, were measured in different solvents and in solid form which is interpreted in Fig. 9. The lifetime of luminescent decay profiles ( ${}^5\text{D}_0$  lifetimes ( $\tau_{\text{obs}}$ )) for the complexes and ligands was the best fitting with mono-exponential curves and measured at room temperature. The observed luminescence decay profile corresponds to a single exponential function, thus implying the presence of only one emissive  $\text{Eu}^{\text{III}}$  centre. The single exponential function is given by the equation  $I(t) = I_0 + A_1 \exp\left(\frac{-t}{\tau}\right)$ , where  $I_0 = 0$  is the offset value,  $A_1$  is the scalar quantity (from curve fitting),  $t$  is the time in

ms and  $\tau$  is the decay time value for the exponential module. The values are suggesting the presence of a single chemical environment around the emitting  $\text{Eu}^{\text{III}}$  ion and compiled in Table 3. The lifetime variations was observed in different solvents and the following order was followed  $\text{CHCl}_3$  (0.67) > Acetone (0.62) > DCM (0.60) > THF (0.59) > DMF (0.50) > solid (0.43ms) for  $\text{Eu}_2(\text{TTA})_6(\text{L1})$  and  $\text{CHCl}_3$  (0.68) > Acetone (0.64) > DCM (0.62) > THF (0.61) > DMF (0.49) > solid (0.42 ms) for  $\text{Eu}_2(\text{TTA})_6(\text{L2})$  at 360 nm. Both the complexes were followed same trend in the solution form towards decreasing of the life time. The highest life time of the solution ( $\text{CHCl}_3$ ) as compared with solid indicates that the non-radiative transition decreases via reducing the vibrational coupling and leads radiative transition enhancement. In addition, the primary process that quenches  $^5\text{D}_0$  excited state of  $\text{Eu}^{\text{III}}$  in solution form by non-radiative relaxation via a vibronic coupling. The excited state life time of  $^5\text{D}_0$  ( $\text{Eu}^{3+}$ ) level ( $\mu\text{s}$  to ms scale) was enable energy transfer by high frequency vibrational oscillators such as O-H, N-H, and C-H and leads to favours quenching of the luminescence. According to the gained results, the C-H vibrational oscillators frequency is less as compare to that of O-H and N-H and  $\text{CHCl}_3$  and DCM are shown enhanced results.

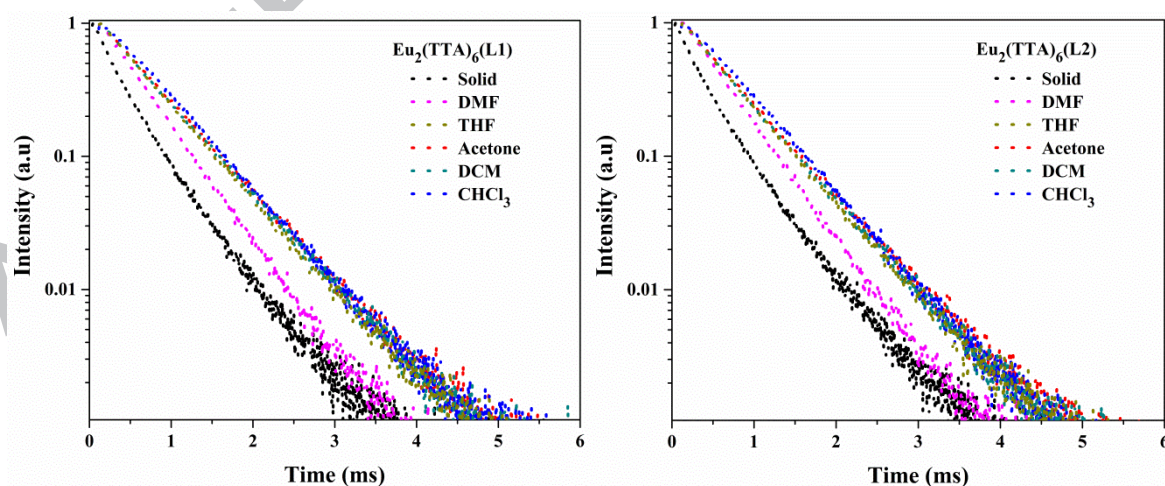


**Fig. 9.** The lifetime of the  $\text{Eu}(\text{III})$  complexes,  $\text{Eu}_2(\text{TTA})_6(\text{L1})$  (left) and  $\text{Eu}_2(\text{TTA})_6(\text{L2})$ (right) in different solvents and in the form of solid.

**Table 3.** The Judd-Ofelt and lifetime analysis of the complexes and ligands in solid form as well as in different solvents.

S. No.	Compound	Intensity Parameters ( $10^{-20} \text{ cm}^2$ )		$\tau / \text{ms}^a$					
		$\Omega_2$	$\Omega_4$	Solid	$\text{CHCl}_3$	DMF	THF	DCM	Acetone
1	$\text{Eu}_2(\text{TТА})_6(\text{L1})$	1.78	0.23	0.43 <sup>b</sup>	0.67	0.50	0.59	0.60	0.62
2	$\text{Eu}_2(\text{TТА})_6(\text{L2})$	2.44	0.24	0.42 <sup>b</sup>	0.68	0.49	0.61	0.62	0.64
3	$\text{L1}(10^{-3} \text{ ms})$ $\lambda_{\text{exc}} 280 \text{ nm}$	---	---	2.11	1.62	1.71	2.10	2.55	1.76
4	$\text{L1}(10^{-3} \text{ ms})$ $\lambda_{\text{exc}} 360 \text{ nm}$	---	---	4.33	11.5	12.0	21.9	23.0	26.8
5	$\text{L2}(10^{-3} \text{ ms})$ $\lambda_{\text{exc}} 280 \text{ nm}$	---	---	1.70	1.85	2.52	1.71	2.51	1.72
6	$\text{L2}(10^{-3} \text{ ms})$ $\lambda_{\text{exc}} 360 \text{ nm}$	---	---	1.92	21.8	24.5	20.6	23.0	20.8

<sup>a</sup>The for the  $\beta$ -diketonate europium(III) complex and its ligand.<sup>b</sup> decay curves were best fitted with bi-exponential curves.

The intrinsic lanthanide quantum yield ( $\Phi_{\text{Ln}}$ ) rationalization in coordination complexes depends on the Judd-Ofelt theory, which considers an odd number of crystal-field contributions. The  $\Phi_{\text{Ln}}$ , experimental branching ratio ( $\beta_{1-3}$ ), stimulated emission cross section ( $\sigma_{1-3}$ ), radiative ( $A_{\text{RAD}}$ ), nonradiative ( $A_{\text{NR}}$ ) decay rates,  $^5\text{D}_0$  lifetime ( $t_{\text{obs}}$ ) and energy transfer efficiency ( $\Phi_{\text{sen}}$ ) parameters were calculated by reported literature [47-50,42,21]. The obtained intrinsic quantum yield ( $\Phi_{\text{Ln}}$ ) and energy transfer efficiency ( $\Phi_{\text{sen}}$ ) indicates that the

currently studied ligand is an efficient sensitizer for  $\text{Eu}^{\text{III}}$  ion in the complexes. The  $\Phi_{\text{sen}}$  is higher for  $\text{Eu}_2(\text{TTA})_6(\text{L2})$  is 91.81 than the complex  $\text{Eu}_2(\text{TTA})_6(\text{L1})$  is 85.14. The obtained higher sensitization is leads to efficient energy transfer and it reveals the higher QY of the  $\text{Eu}_2(\text{TTA})_6(\text{L2})$ . In addition, radiative and non-radiative transitions can be expressed by radiative rate constants, which are available from emission lifetimes and the quantum yields. As know the relation between  $\Phi_f$  and  $\tau$ , if  $\Phi_f$  is high and  $\tau$  is also extended. In case the compounds are non-fluorescent, the lifetime are estimated to be very short and it indicate the very fast decay. The rate constants are calculated by  $R = \Phi_f/\tau$  and the values are  $7.395 \times 10^{-4} \text{ s}^{-1}$ ,  $7.714 \times 10^{-4} \text{ s}^{-1}$  found for  $\text{Eu}_2(\text{TTA})_6(\text{L1})$ ,  $\text{Eu}_2(\text{TTA})_6(\text{L2})$ , respectively [51]. The comparative radiative constants of the complexes are not much varied and since their life time also almost similar. Rapid decay due to large nuclear distortion leads to decrease the quantum yield and reflects the R value also decreases. In addition, the  $\text{Eu}_2(\text{TTA})_6(\text{L2})$  shown comparatively high R and it reveals less nuclear distortions between the ground and the first excited singlet state. The detailed calculated parameters are tabulated in Table 4 and Table 5.

**Table 4.** Experimental branching ratios ( $\beta_{1-3}$ ) and stimulated emission cross section ( $\sigma_{1-3}$ ) of the complex.

S. No.	Complex name	$\sigma_1$	$\sigma_2$	$\sigma_3$	$\beta_1$	$\beta_2$	$\beta_3$
1.	$\text{Eu}_2(\text{TTA})_6(\text{L1})$	0.520	6.935	0.336	7.92	86.65	5.42
2.	$\text{Eu}_2(\text{TTA})_6(\text{L2})$	0.505	1.117	0.329	5.96	89.82	4.24

**Table 5.** The Radiative ( $A_{\text{RAD}}$ ) and nonradiative ( $A_{\text{NR}}$ ) decay rates,  $^5\text{D}_0$  lifetime ( $t_{\text{obs}}$ ), intrinsic quantum yield ( $\Phi_{\text{Ln}}$ ), energy transfer efficiency ( $\Phi_{\text{sen}}$ ) and overall quantum yield ( $\Phi_{\text{overall}}$ ) for the complex.

S. No.	Complex name	$A_{\text{RAD}}$ ( $\text{S}^{-1}$ )	$A_{\text{NR}}$ ( $\text{S}^{-1}$ )	$\tau_{\text{obs}}$ (ms)	$\tau_{\text{RAD}}$ (ms)	$\Phi_{\text{Ln}}$ (%)	$\Phi_{\text{Sen}}$ (%)	$\Phi_{\text{Overall}}$ (%)
1.	$\text{Eu}_2(\text{TTA})_6(\text{L1})$	630.681	170	0.43	1.59	27.04	85.14	31.8
2.	$\text{Eu}_2(\text{TTA})_6(\text{L2})$	838.937	154	0.42	1.19	35.29	91.81	32.4

### Electrochemical Properties

The electrochemical properties were carried out for newly synthesized ligands and the corresponding binuclear complexes and shown in Fig. 10. From the voltammogram, the oxidation potentials of the ligands (L1 and L2) and complexes ( $\text{Eu}_2(\text{TTA})_6(\text{L1})$  and  $\text{Eu}_2(\text{TTA})_6(\text{L2})$ ) were found to be 1.38, 1.27 and 1.45, 1.39 eV, respectively. The obtained oxidation potentials from the CV analysis and other values are tabulated in Table 6. The obtained oxidation potentials of the complexes were decreased as compared to that of ligand. A similar observation was also been seen in case of reduction potential. The followed equation which is reported by de Leeuw *et al.*, [52] used to calculate the HOMO and LUMO energy levels.

$$E_{\text{HOMO}} = - (E_{\text{onset} \rightarrow \text{SCE}}^{\text{Oxi}} + 4.4) \text{ eV}$$

$$E_{\text{LUMO}} = - (E_{\text{onset} \rightarrow \text{SCE}}^{\text{Red}} + 4.4) \text{ eV}$$

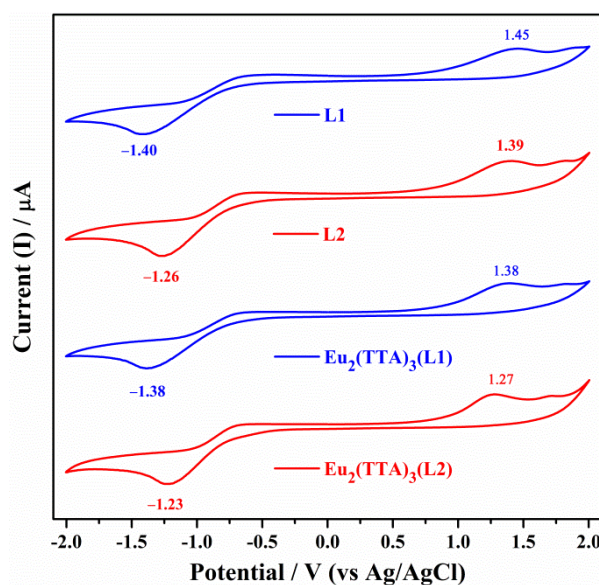


**Fig. 10.** Cyclic voltammogram of ligands and its corresponding Eu(III)-complexes.

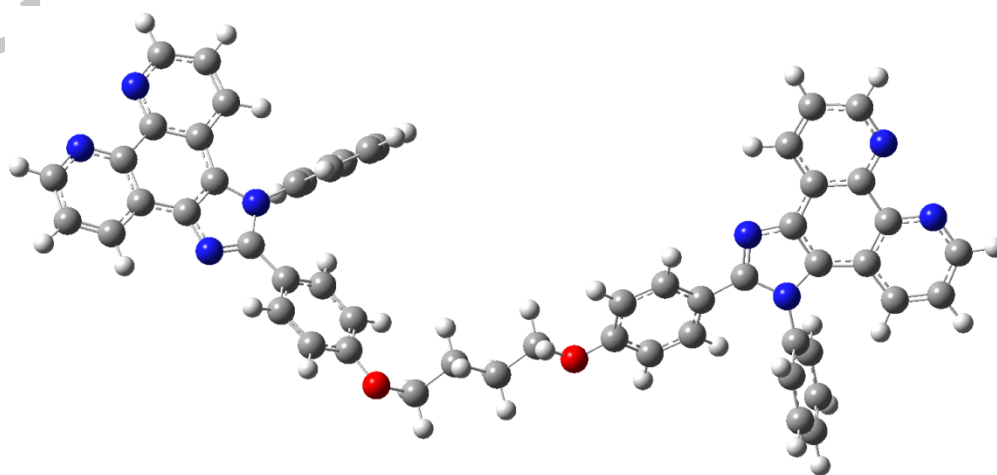
**Table 6.** Electrochemical properties of the ligands and respective Eu(III)-complexes.

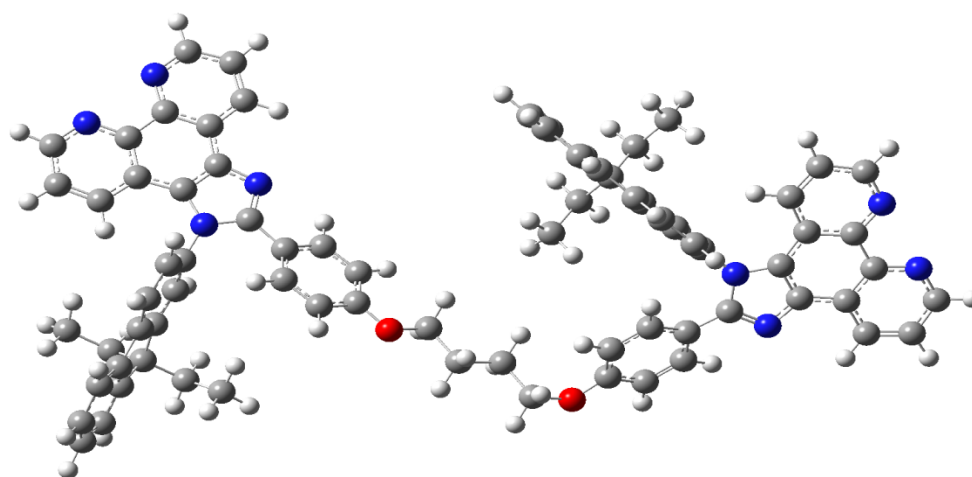
S.No.	Compound Name	Voltage <sub>onset</sub> <sup>Oxi</sup> [V] ( $E_{\text{HOMO}}$ [eV])	Voltage <sub>onset</sub> <sup>Red</sup> [V] ( $E_{\text{LUMO}}$ [eV])	$\lambda_{\text{onset}}$ [nm](a)	Band gap/Energy gap $E_g^{\text{Opt}}$ , [eV] (b)
1.	<b>Eu<sub>2</sub>(TTA)<sub>6</sub>(L1)</b>	1.38 (-5.78)	-1.38 (-3.02)	452.4	2.74 (2.76)
2.	<b>Eu<sub>2</sub>(TTA)<sub>6</sub>(L2)</b>	1.27 (-5.67)	-1.23 (-3.17)	459.2	2.70 (2.50)
3.	<b>L1</b>	1.45 (-5.85)	-1.40 (-3.00)	411.9	3.01(2.85)
4.	<b>L2</b>	1.39 (-5.79)	-1.26 (3.14)	454.1	2.73 (2.65)

$E_{\text{red}}^{\text{onset}}$  = the onset reduction potentials,  $E_{\text{oxd}}^{\text{onset}}$  = the onset oxidation potentials,  $E_g$  = band gap,  $E_g = E_{\text{LUMO}} - E_{\text{HOMO}}$ . [a] Calculated from the optical absorption (DRS spectra), [b] Calculated the onset wavelength of optical absorption (onset) in solid-state film (DRS spectra). The energy differences (HOMO and LUMO) values calculated by cyclic voltammogram are mentioned in bracket.

The calculated optical energy gap (DRS spectral analysis) of the ligands as well as complexes was similar to that of the results obtained from the electrochemical

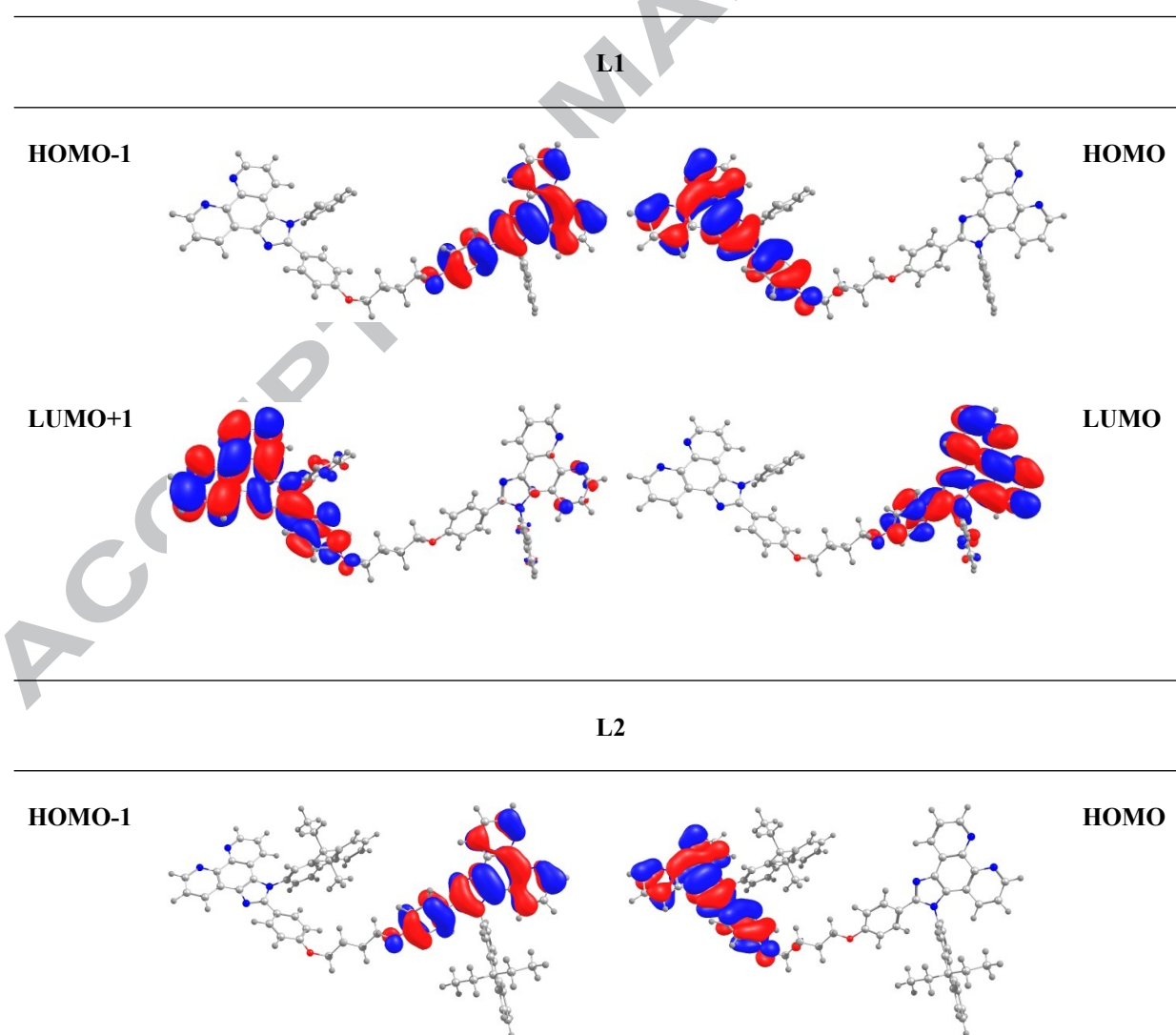
analysis. The overall band gap of the complexes was less as compared with the respective ligands. The TPA based complex energy gap is slightly higher than that of currently synthesized complexes. These results are suggesting that the spacer arrangement can be a better choice to get suitable energy distance. The L2 consist less energy gap than L1 ligand and it is suitable to harvest the efficient energy from the Eu-complex. Similarly, the complex ( $\text{Eu}_2(\text{TTA})_6(\text{L2})$ ) gained less energy gap and more suitable to get efficient energy transfer. Since the efficient energy transfer process needs acceptor ( $^5\text{D}_0$ ) energy level should be lesser than the donor (ligand). This criteria very much can full filled by  $\text{Eu}_2(\text{TTA})_6(\text{L2})$  complex. The energy gap calculations were made by theoretical calculations and the calculated HOMO-LUMO energy levels by theoretically is similar to the observations made in the experimental (calculated from the optimized structure, Fig. 11) [53-56] and xyz coordinates of the ligands L1 and L2 are incorporated in Fig. S5. The calculated molecular orbitals of the ligands L1 and L2 electron density is located on phenanthro-imidazole ring and on Ph/Fluorene (some amount transferred to imidazole moiety) moiety for HOMO and LUMO, respectively (Table 7) and their respective values were mentioned in Table 8. In addition, the computed vertical transitions, as well as their oscillator strengths and configurations of ligands (L1 and L2), were also incorporated in Table S4.





**Fig. 11.** The optimized ligands, L1 (up) and L2 (down) structures by theoretical analysis.

**Table 7.** The HOMO and LUMO energy levels of the ligand.



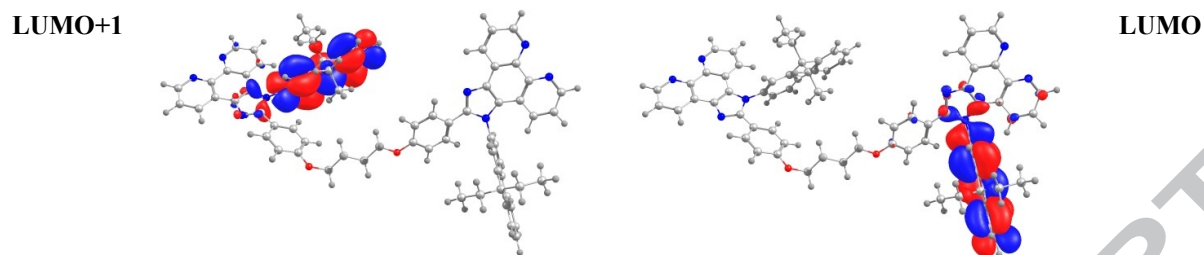


**Table 8.** The HOMO and LUMO energy levels of the ligands.

Molecule	HOMO	HOMO-1	LUMO	LUMO+1	$E_g$	S1	T1
	in electron volts (eV)						
<b>L1</b>	-5.40	-5.35	-1.22	-1.18	4.13	3.59	2.75
<b>L2</b>	5.31	5.36	1.43	1.42	3.87	3.36	2.74
<b>Eu<sub>2</sub>(TTA)<sub>6</sub>(L1)</b> <b>Eu<sub>2</sub>(TTA)<sub>6</sub>(L2)</b>	---	---	---	---	---	<sup>5</sup> D <sub>0</sub> level = 2.17	

### CIE Chromaticity coordinates

The Commission Internationale de l'Eclairage (CIE) values of the bipolar ligand and the respective binuclear complexes were calculated from the PL emission spectra in solution as well as solid state (Fig. 12). The calculated CIE values are tabulated in Table 9. The ligand is shown blue emission in solution but in the case of the solid state, it was shifted towards sky blue and greenish white emission. By molecular structure engineering (by functionalizing or changing the substitutes in the back bone of the ligand), it is possible to generate white light emissive single molecular emitters. The complex was shown red emission with apt CIE color coordinate values and almost identical to the CIE value of the pure red emission designated by the national television standard committee (NTSC). The optimizations of the ligand structures are in progress in our laboratories, to obtain pure white (near) emissions.

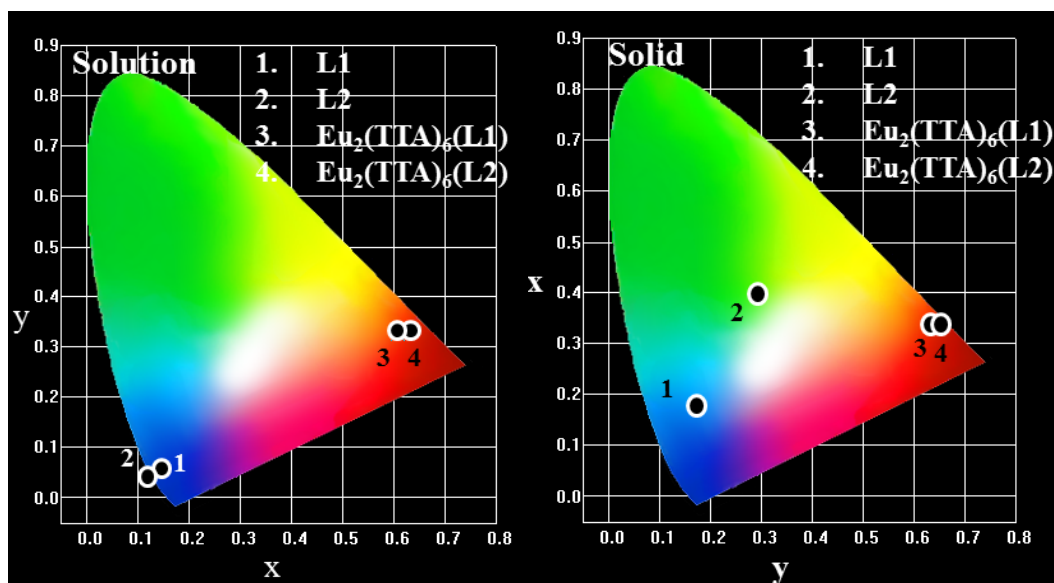


**Fig. 12.** The CIE chromaticity coordinates for bipolar ligands and binuclear Eu-complexes in solution (left) and solid (right).

**Table 9.** The CIE color coordinates for the bipolar ligands and binuclear Eu(III) complexes.

S.No.	Compound Name	Solution (a)(b)		Solid (b)	
		x	y	x	Y
1	$\text{Eu}_2(\text{TTA})_6(\text{L1})$	0.61	0.33	0.63	0.33
2	$\text{Eu}_2(\text{TTA})_6(\text{L2})$	0.63	0.33	0.65	0.34
3	$\text{Eu}(\text{TTA})_3 \cdot 2\text{H}_2\text{O}$	0.66	0.33	0.65	0.33
4	L1	0.16	0.06	0.17	0.18
5	L2	0.11	0.05	0.29	0.40

[a] Measured in chloroform solution at 298 K, [b] Emission peaks from PL emission spectra.

### PMMA film of binuclear Eu(III) complexes

In order to gain more information about the optical properties of Eu-complex in a matrix, the complex was also dispersed in PMMA matrix and their PL emission spectra, respective digital photographs are shown in Fig. 13. The PL emission of the thin film was made in different concentrations which are 0.1, 0.5, 1 and 5 % doping of

complex with PMMA. The excitation maxima were observed at ~360 nm and shown in Fig. S8 and S9. As compared with the complex in the pure situation on a glass substrate shown less intensity peaks than PMMA doped thin films. However, all the percentage of the thin films was shown best characteristic pure red emission and satisfying the NTSC standards ( $x = 0.66$ ,  $y = 0.33$ ). In addition, the FWHM and intensity ratios were also calculated to understand the emission as well as the symmetry of the complexes (Table S3). The FWHM of the complexes was found to be very narrow which is almost 4 nm. It is better as compared with a solution and solid phase. The calculated intensity ratios of complexes were shown approximately 20 ( $I_2 / I_1$ ), which is clearly indicating that the Eu metal ion occupied non-center of symmetry and experienced more unsymmetrical. A thin film of the intensity parameter value is higher than the solution and solid, which also signifying that the currently synthesized complexes are better achiever to get the efficient pure red luminescence. It is also worth to note that the thin film of the QY was also improved than the solution and solid. The detailed calculated CIE, FWHM and intensity ratios were incorporated in the Table S3. These results conclude that the energy transfer from the ligand to center europium (III) metal ion is very efficient in presently discussed complexes. The pictorial view of the CIE color coordination location in the CIE color grout is shown in Fig. S10.

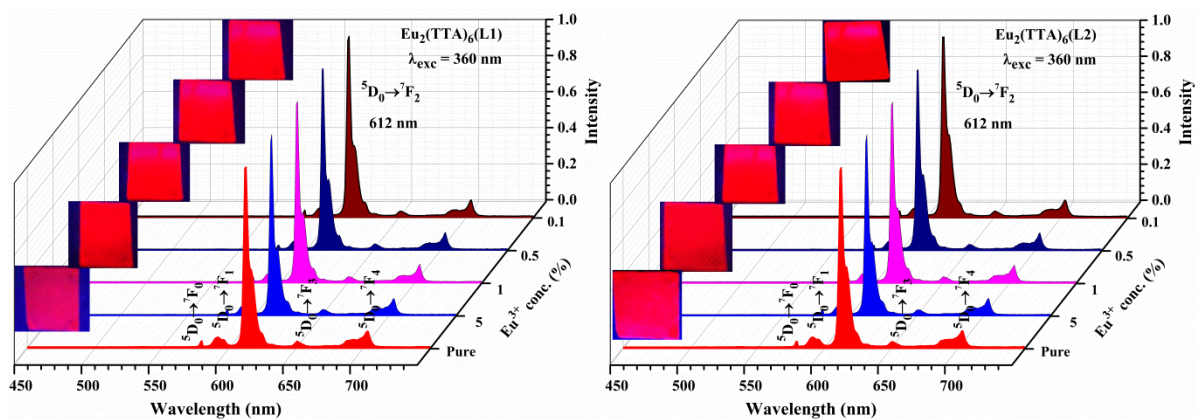


**Fig.13.** The emission spectra of Eu(III) complexes (left-L1, right-L2) doped with PMMA (different percentage ratio) as well as pure Eu(III) complex.

#### Fabrication of LED with Eu complexes:

The combination of a 395 nm emitting InGaN chip with the complexes in different ratios like 1:10 and 1:50 (Eu(III) complex: PMMA) are made to use light-emitting diodes for the complexes. The fabricated LEDs were glowing under 20 mA forward-bias current. The emission of the complexes was shown intensive emission peak at 612 nm. The excitation source of the LED is almost transferred to the complex,  $\text{Eu}_2(\text{TTA})_6(\text{L}2)$  and it is less in rest of the complex (Fig. 14). However, both the complexes are shown efficient red emission with CIE are  $x = 0.65, y = 0.34$  (1:10);  $x = 0.66, y = 0.34$  (1:50) and 2Eu is  $x = 0.66, y = 0.33$  (1:10);  $x = 0.66, y = 0.33$  (1:50), respectively. These results are indicating that the presently synthesized complexes are best materials for red emitting LEDs. The LED CIE color coordinates for the  $\text{Eu}^{\text{III}}$  complexes in different ratio were shown in Fig. S11.

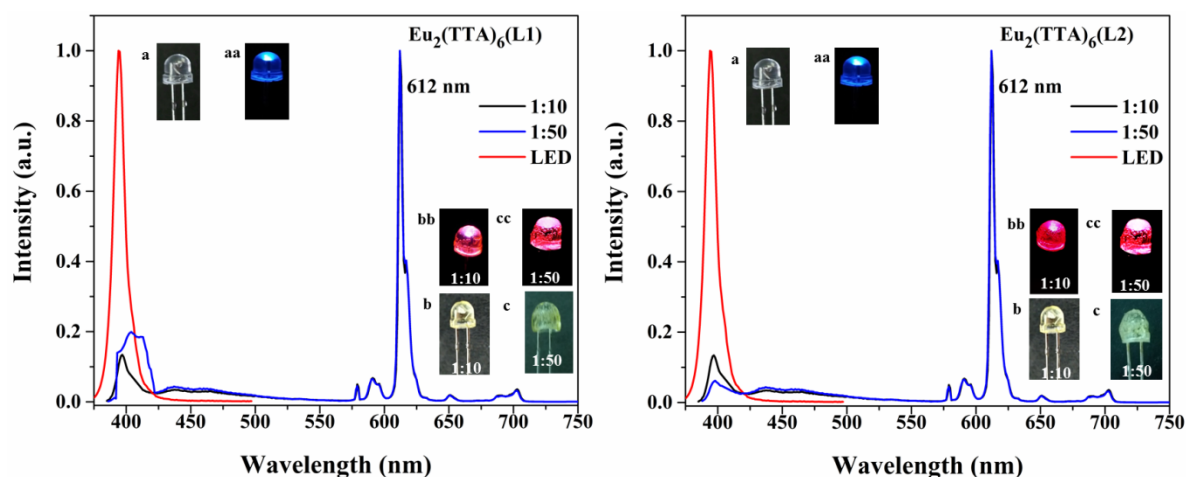


**Fig. 14.** The spectra's of Eu(III) complexes coated on the 395 nm emitted LED (InGaN) chip. In inset **a** is the original 365 nm emitted LED chip, **aa** is under forward bias. **b** and **c** are coated with binuclear Eu(III) complexes and **bb** and **cc** are with forward bias, respectively.

## Conclusion

The ligand with spacer moiety for binuclear complexes was designed and synthesized successfully. The PL emission spectral study of the ligands shown blue to greenish white (solution to solid) and their respective complexes showed efficient characteristic red emission and there is no emission additional emission in the region of 400-550 nm. The calculated sensitizer parameters shown currently synthesized ligands are good sensitizers for Eu<sup>III</sup> metal ion. It reveals that in the complex fully energy transfer from ligand to Eu metal ion and the same was also confirmed by DFT and TD-DFT calculations. The obtained highest QY (59.5 %) of the thin film the complex, Eu<sub>2</sub>(TTA)<sub>6</sub>(L2) indicating efficient energy sensitization from fluorene-based ligand than in rest of the complex. The narrow emission width of the complexes indicates that the synthesized complexes are red efficient. The improved intensity of the thin film than the solution and solid clearly indicating that the Eu metal ion occupies the strong on-center of symmetry leads pure red emission; clear by CIE coordinates. The fabricated LED conjugated with Eu-complex shown red efficient. These observations are indicating that the presently synthesized complexes are potential lighting sources.

## Acknowledgments

The authors gratefully thank for the financial support from the Board of Research in Nuclear Sciences (BRNS), Department of Atomic Energy (DAE), INDIA.

## References

1. J. C. G. Bunzli, S. V. Eliseeva, Lanthanide NIR luminescence for telecommunications, bioanalyses and solar energy conversion, *J. Rare Earths* 28 (2012) 824–842.
2. X. Huang, S. Han, W. Huang, X. Liu, Enhancing solar cell efficiency: the search for luminescent materials as spectral converters, *Chem. Soc. Rev.* 42 (2013) 173–201.
3. S. Liu, P. He, H. Wang, J. Shi, M. Gong, pH-induced molecular switch of a novel trinuclear Ru(II) polypyridyl complex, *Inorg. Chem. Commun.* 12 (2009) 506–508.
4. T. Yayamura, S. Iwata, S. Iwamaru, H. Tomiyasu, Effect of complexation on the excited state of uranyl  $\beta$ -diketonato complexes: applications of the energy gap law, *J. Chem. Soc. Faraday Trans.* 90 (1994) 3253–3259.
5. J. Feng, H. Zhang, Hybrid materials based on lanthanide organic complexes: a review, *Chem. Soc. Rev.* 42 (2013) 387–410.
6. J. C. G. Bunzli, Lanthanide luminescence for biomedical analyses and imaging, *Chem. Rev.* 110 (2010) 2729–2755.
7. K. S. Kumar, B. Schafer, S. Lebedkin, L. Karmazin, M. M. Kappes, M. Ruben, Highly luminescent charge-neutral europium(III) and terbium(III) complexes with tridentate nitrogen ligands, *Dalton Trans.* 44 (2015) 15611–15619.
8. Y. Liu, Y. Wang, H. Guo, M. Zhu, C. Li, J. Peng, W. Zhu, Y. Cao, Synthesis and optoelectronic characterization of a monochromic red-emitting europium(III) complex

- containing triphenylamine-functionalized phenanthroline, *J. Phys. Chem. C* 115 (2011) 4209–4216.
9. M. Latva, H. Takalo, V. M. Mikkala, C. Matachescu, J. C. Rodriguez-Ubis, J. Kankare, Correlation between the lowest triplet state energy level of the ligand and lanthanide(III) luminescence quantum yield, *J. Lumin.* 75 (1997) 149–169.
10. A. De Bettencourt-Dias, P. S. Barber, S. Viswanathan, Aromatic N-donor ligands as chelators and sensitizers of lanthanide ion emission, *Coord. Chem. Rev.* 273–274 (2014) 165–200.
11. B. Rajamouli, Rachna Devi, Abhijeet Mohanty, Venkata Krishnan, V. Sivakumar, Effects of electron withdrawing groups in imidazole-phenanthroline ligands and their influence on photophysical properties of  $\text{Eu}^{\text{III}}$  complexes for white light emitting diodes, *New J. Chem.* 41 (2017) 9826–9839.
12. S. Kasturi, B. Rajamouli, V. Sivakumar, Versatile luminescent Europium(III)- $\beta$ -diketonate-imidazo-bipyridyl complexes intended for white LEDs: A detailed photophysical and theoretical study, *Inorg. Chem.* 56 (2017) 9376–9390.
13. Rashid Ilmi, Ashanul Haque, M. S. Khan., Synthesis and photo-physics of red emitting europium complexes: An estimation of the role of ancillary ligand by chemical partition of radiative decay rate, *Journal of Photochemistry and Photobiology A: Chemistry* 370 (2019) 135-144.
14. C. Q. Shen, T. L. Yan, Y. T. Wang, Z. J. Ye, W. J. Zhou, Synthesis, structure and luminescence properties of binary and ternary complexes of lanthanide ( $\text{Eu}^{3+}$ ,  $\text{Sm}^{3+}$  and  $\text{Tb}^{3+}$ ) with salicylic acid and 1,10-phenanthroline, *J. Lumin.* 184 (2017) 48–54.
15. L. Wang, Z. Jun, L. Ni, J. Yao, Synthesis, structures, fluorescence properties, and natural bond orbital (NBO) analysis of two metal [ $\text{Eu}^{\text{III}}$ ,  $\text{Co}^{\text{II}}$ ] coordination polymers

- containing 1,3-benzenedicarboxylate and 2-(4-methoxyphenyl)-1H-imidazo[4, 5-f][1, 10]phenanthroline ligands, *Z. Anorg. Allg. Chem.* 638 (2012) 224–230.
16. Y. Haas, G. Stein, Pathways of radiative and radiationless transitions in europium(III) solutions. Role of solvents and anions, *J. Phys. Chem.* 75 (1971) 3668–3677.
17. Y. Haas, G. Stein, Pathways of radiative and radiationless transitions in europium(III) solutions. The role of high energy vibrations, *J. Phys. Chem.* 75 (1971) 3677–3681.
18. B. Rajamouli, C. S. D. Viswanath, S. Giri, C. K. Jayasankar, V. Sivakumar, Carbazole functionalized new bipolar ligand for monochromatic red light emitting europium(III) complex: combined experimental and theoretical study, *New J. Chem.* 41 (2017) 3112–3123.
19. B. Rajamouli, K. Singh, S. Giri, V. Sivakumar, Controlled energy transfer from ligand to Eu(III) ion: A unique strategy to obtain bright white light emission and their versatile applications, *Inorg. Chem.* 56 (2017) 10127–10130.
20. B. Rajamouli, P. Sood, S. Giri, V. Krishnan, V. Sivakumar, New dual characteristic bidentate ligand for ternary mono nuclear europium(III) molecular complex: synthesis, photophysical, electrochemical and theoretical study, *Eur. J. Inorg. Chem.* 24 (2016) 3900–3911.
21. B. Rajamouli, V. Sivakumar, Effect of carbazole functionalization with a spacer moiety in the phenanthroimidazole bipolar ligand in a europium(III) complex on its luminescence properties: combined experimental and theoretical study, *New J. Chem.* 41 (2017) 1017-1027.
22. B. Rajamouli, V. Sivakumar, Carbazole and fluorene functionalized phenanthroimidazole ancillary ligand based Eu(III) complexes for LEDs: Detailed photophysical and theoretical study, *Chemistry Select* 1 (2017) 1-13.

23. X. F. Zhang, C. J. Xu, J. Wan, Mono- and dinuclear europium(III) complexes with thenoyltrifluoroacetone and 1,10-phenanthroline-5,6-dione, *Monatsh Chem.* 145 (2014) 1913–1917.
24. H. Jang, C. H. Shin, B. J. Jung, D. Kim, H. K. Shim, Y. Do, Synthesis and characterization of dinuclear europium complexes showing pure red electroluminescence, *Eur. J. Inorg. Chem.* (2006) 718–725.
25. T. Cardinaels, K. Driesen, T. N. Parac-Vogt, B. Heinrich, C. Bourgogne, D. Guillon, B. Donnio, K. Binnemans, Design of high coordination number metallomesogens by decoupling of the complex-forming and mesogenic groups: nematic and lamello-columnar mesophases, *Chem. Mater.* 17 (2005) 6589–6598.
26. A. P. Bassett, S. W. Magennis, P. B. Glover, D. J. Lewis, N. Spencer, S. Parsons, R. M. Williams, L. De Cola, L. Pikramenou, Highly luminescent, triple- and quadruple-stranded, dinuclear Eu, Nd, and Sm(III) lanthanide complexes based on bis-diketonate ligands, *J. Am. Chem. Soc.* 126 (2004) 9413–9424.
27. M. Irfanullah, K. Iftikhar, New dinuclear lanthanide(III) complexes based on 6,6,7,7,8,8,8-heptafluoro-2,2-dimethyl-3,5-octanedione and 2,2'-bipyrimidine, *Inorg. Chem. Commun.* 12 (2009) 296–299.
28. C. L. Yang, J. X. Luo, J. Y. Ma, L. Y. Liang, M. G. Lu, Highly quantum efficiency trinuclear  $\text{Eu}^{3+}$  complex based on tris-diketonate ligand, *Inorg. Chem. Commun.* 14 (2011) 61–63.
29. C. L. Yang, J. X. Luo, J. Y. Ma, M. G. Lu, L. Y. Liang, B.-H. Tong, Synthesis and photoluminescent properties of four novel trinuclear europium complexes based on two tris- $\beta$ -diketones ligands, *Dyes Pigm.* 92 (2012) 696–704.

30. C. Yang, J. X. Jianying Ma, D. Zhu, Y. Zhang, L. Liang, M. Lu, The effect of two additional  $\text{Eu}^{3+}$  lumophors in two novel trinuclear europium complexes on their photoluminescent properties, *Photochem. Photobiol. Sci.* 12 (2013) 330.
31. H. Xu, Q. Sun, Z. An, Y. Wei, X. Liu, Electroluminescence from europium(III) complexes, *Coord. Chem. Rev.* 293–294 (2015) 228–249.
32. A. Pana, F. L. Chiriac, M. Secu, I. Pasuk, M. Ferbinteanu, M. Micutz, V. Circu, A new class of thermotropic lanthanidomesogens:  $\text{Eu(III)}$  nitrate complexes with mesogenic 4-pyridone ligands, *Dalton Trans.* 44 (2015) 14196–14199.
33. S. Dehn, K. W. K. Tong, R. G. C. Clady, D. M. Owen, K. Gaus, T. W. Schmidt, F. Braet, P. Thordarson, The structure and luminescence properties of europium(III) triflate doped self-assembled pyromellitimide gels, *New J. Chem.* 35 (2011) 1466–1471.
34. S. Li, G. Zhong, W. Zhu, F. Li, J. Pan, W. Huang, H. Tian, Dendritic europium complex as a single dopant for white-light electroluminescent devices, *J. Mater. Chem.* 15 (2005) 3221–3228.
35. C. Yang, S. Liu, J. Xu, Y. Li, M. Shang, L. Lei, G. Wang, J. He, X. Wang, M. Lu, Efficient red emission from poly(vinyl butyral) films doped with a novel europium complex based on a terpyridyl ancillary ligand: synthesis, structural elucidation by Sparkle/RM1 calculation, and photophysical properties, *Polym. Chem.* 7 (2016) 1147–1157.
36. Y. Liu, Y. Wang, H. Guo, M. Zhu, C. Li, J. Peng, W. Zhu, Y. Cao, Synthesis and optoelectronic characterization of a monochromic red-emitting Europium(III) complex containing triphenylamine-functionalized phenanthroline, *J. Phys. Chem. C* 115 (2011) 4209–4216.
37. H. Xu, K. Yin, W. Huang, Novel light-emitting ternary  $\text{Eu}^{3+}$  complexes based on multifunctional bidentate aryl phosphine oxide derivatives: Tuning photophysical and

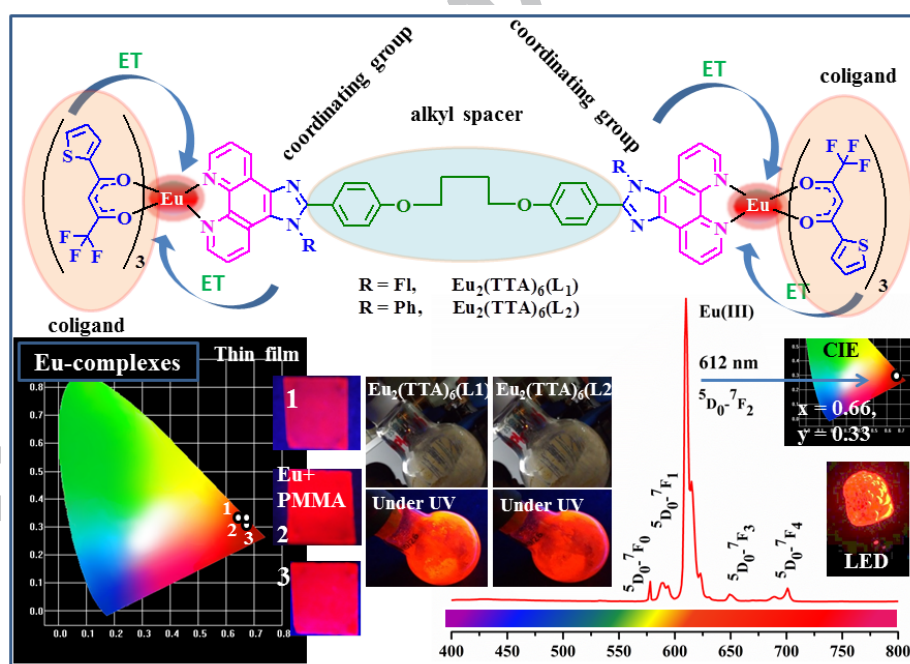
- electrochemical properties toward bright electroluminescence, *J. Phys. Chem. C* 114 (2010) 1674–1683.
38. K. Singh, S. Vaidyanathan,  $\text{Eu}^{2+}$  luminescence in  $\text{Ca}_3\text{Si}_2\text{O}_7$  and spectral widening and tuning of  $\text{Eu}^{2+}$  emission color (orangish-red to green) by crystal chemical substitution, *RSC Advances*.6 (2016) 98652-98662.
39. C. B. Murphy, Y. Zhang, T. Troxler, V. Ferry, J. J. Martin, W. E. Jones, Probing Förster and Dexter energy-transfer mechanisms in fluorescent conjugated polymer chemosensors, *J. Phys. Chem. B* 108 (2004) 1537–1543.
40. D. L. Dexter, A theory of sensitized luminescence in solids, *J. Chem. Phys.* 21 (1953) 836–850.
41. E. Nakazawa, in *Phosphor Handbook*, ed. S. Shionoya, W. M. Yen, H. Yamamoto, CRC Press, Boca Raton, 2007, 2nd edn.
42. A. R. Ramya, M. L. P. Reddy, A. H. Cowley, K. V. Vasudevan, Synthesis, crystal structure, and photoluminescence of homodinuclear lanthanide 4-(Dibenzylamino)benzoate complexes, *Inorg. Chem.* 49 (2010) 2407-2415.
43. E. G. Moore, A. P. S. Samuel, K. N. Raymond, From antenna to assay: Lessons learned in lanthanide luminescence, *Acc. Chem. Res.* 42 (2009) 542.
44. K. Binnemans, Interpretation of europium(III) spectra, *Coord. Chem. Rev.* 295 (2015) 1–45.
45. F. J. Steemers, W. Verboom, D. N. Reinhoudt, E. B. V. Tol, J. W. Verhoeven, New Sensitizer-Modified Calix[4]arenes Enabling Near-UV Excitation of Complexed Luminescent Lanthanide Ions, *J. Am. Chem. Soc.* 117 (1995) 9408–9414.
46. S. J. L. Ribeiro, R. E. O. Diniz, Y. Messaddeq, L. A. Nunes, M. A. Aegerter,  $\text{Eu}^{3+}$  and  $\text{Gd}^{3+}$  spectroscopy in fluorindate glasses, *Chem. Phys. Lett.* 220 (1994) 214–218.

47. J. C. G. Bunzli, A. S. Chauvin, H. K. Kim, E. Deiters, S. V. Eliseeva, Lanthanide luminescence efficiency in eight- and nine-coordinate complexes: Role of the radiative lifetime, *Coord. Chem. Rev.* 254 (2010) 2623–2633.
48. W. T. Carnall, In *Handbook on the Physics and Chemistry of Rare Earths*, Eds. K. A. Gschneidner and L. Eyring, North-Holland Publishing Co., Amsterdam, 3 (1979) 171–208.
49. Raif Hermann, Reiner Mehnert, Laszlo Wojnarovits, Fluorescence lifetimes and radiative rate constants of alkanes at 25°C, *J. Lumin.* 33 (1985) 69-78.
50. C. G. Walrand, K. Binnemans, In *Handbook on the Physics and Chemistry of Rare Earths*, Eds. K. A. Gschneidner and L. Eyring, Elsevier Science: Amsterdam 25 (1998) 101–264.
51. C. Reinhard, H. U. Gudel, High-resolution optical spectroscopy of  $\text{Na}_3[\text{Ln}(\text{dpa})_3] \cdot 13\text{H}_2\text{O}$  with  $\text{Ln} = \text{Er}^{3+}, \text{Tm}^{3+}, \text{Yb}^{3+}$ , *Inorg. Chem.* 41 (2002) 1048–1055.
52. D. M. de Leeuw, M. M. J. Simenon, A. R. Brown, R. E. F. Einerhand, Stability of n-type doped conducting polymers and consequences for polymeric microelectronic devices, *Synth. Met.* 87 (1997) 53–59.
53. H. Li, Y. Wang, K. Yuan, Y. Tao, R. Chen, C. Zheng, X. Zhou, J. Li, W. Huang, Efficient synthesis of  $\pi$ -extended phenazasilines for optical and electronic applications, *Chem. Commun.* 50 (2014) 15760.
54. M. M. Nolasco, P. D. Vaz, L. D. Carlos, The role of 4,7-disubstituted phenanthroline ligands in energy transfer of europium(III) complexes: a DFT study, *New J. Chem.* 35 (2011) 2435.
55. S. Yoo, X. C. Zeng, S. S. Xantheas, On the phase diagram of water with density functional theory potentials: The melting temperature of ice Ih with the Perdew–Burke Ernzerhof and Becke–Lee–Yang–Parr functionals, *J. Chem. Phys.* 130 (2009) 221102.

56. B. Komjati, A. Urai, S. Hosztafi, J. Kokosi, B. Kovats, J. Nagy, P. Horvath, Systematic study on the TD-DFT calculated electronic circular dichroism spectra of chiral aromatic nitro compounds: A comparison of B3LYP and CAM-B3LYP, Spectrochim. Acta Mol. Biomol. Spectrosc.155 (2016) 95–102.

## TOC

The strategy of structure and photoluminescence emission spectral study was shown dominant electric dipole transition of  $\text{Eu}^{\text{III}}$  ion ( $^5\text{D}_0 \rightarrow ^7\text{F}_2$ , 612 nm) and their digital images under normal as well as UV light. The binuclear Eu-complexes were combined with InGaN near UV LED, obtained pure red emission (forward bias 20 mA) with CIE color coordinate values  $x = 0.66$ ,  $y = 0.33$ .



57.

## Highlights

- ✓ Two newly designed and synthesized ancillary ligands with N1 functionalization (phenyl and fluorene) and their binuclear europium complexes were investigated systematically.

- ✓ The absorption spectra of the ligands show expected absorption due to  $\pi$ - $\pi^*$  transition of the aromatic ring (confirmed by theoretical calculation).
- ✓ Photoluminescence emission spectral study shown the efficient energy transfer from ligand to central  $\text{Eu}^{\text{III}}$  ion in the complex and confirmed by experimentally and TD-DFT calculations.
- ✓ The obtained highest QY (59.5 %, thin film) of the complex,  $\text{Eu}_2(\text{TTA})_6(\text{L2})$  indicating efficient energy sensitization from fluorene-based ligand than that of phenyl based Eu-complex.
- ✓ The binuclear Eu-complexes were combined with InGaN near UV LED, obtained pure red emission with CIE color coordinate value  $x = 0.66, y = 0.33$ .

58.